GLOBAL OPTIMIZATION FOR THE PHASE AND CHEMICAL EQUILIBRIUM PROBLEM: APPLICATION TO THE NRTL EQUATION

Conor M. McDonald and Christodoulos A. Floudas*
Department of Chemical Engineering
Princeton University
Princeton, N.J. 08544-5263

Submitted September 7, 1993; revised August 10, 1994;
Accepted by *Comp. & chem. eng.*

Abstract

Several approaches have been proposed for the computation of solutions to the phase and chemical equilibrium problem when the problem is posed as the minimization of the Gibbs free energy function. None of them can guarantee convergence to the *true* optimal solution, and are highly dependent on the supplied initial point. Convergence to local solutions often occurs, yielding incorrect phase and component distributions. This work examines the problem when the liquid phase is adequately modeled by the Non-Random Two Liquid (NRTL) activity coefficient expression and the vapor phase is assumed to be ideal. The contribution of the proposed approach is twofold. Firstly, a novel and important property of the Gibbs free energy expression involving the NRTL equation is provided. It is subsequently shown that by introducing new variables, the problem can then be transformed into one where a biconvex objective function is minimized over a set of bilinear constraints. Secondly, the Global OPtimization (GOP) algorithm (Floudas and Visweswaran, [13, 14]; Visweswaran and Floudas, [60, 61, 62]) is used to exploit these induced properties of the formulation to guarantee convergence to an ϵ-global solution, regardless of the starting point. A geometrical interpretation is provided for a selected smaller, but challenging, example. Numerous examples are presented which demonstrate the broad applicability of the proposed approach.

*Author to whom all correspondence should be addressed.

1 Introduction

The separation of fluid mixtures is a fundamental aspect of chemical process design. To accomplish it effectively reliable thermodynamic models are required to describe the chemical and phase equilibrium between these fluids. Even when such models are available, problems may arise in attempting to predict or estimate the number and type of phases, and the distribution of components within them at equilibrium due to the possible unreliability of experimental data or the potential inadequacy of the equilibrium models at hand.

A considerable literature has been generated on approaches to this problem. These divide into two broad classifications. The first is equation based and is generally referred to as the stoichiometric approach. Early work in this area, such as that of Brinkley [4], concentrated on solving the set of nonlinear algebraic equations based on the equilibrium constant expressions and the material balance equations. Sanderson and Chien [50] solved these equations using Marquardt's [32] method after reformulating the problem into an unconstrained nonlinear form. Xiao *et al.* [66] improved the algorithm of Sanderson and Chien [50] by modifying the procedure with which the inner and outer iteration loops are solved. These k-value methods are especially suited to certain classes of problems that are not under consideration in this work. The book of Smith and Missen [52] provides a thorough review and exposition of the work accomplished in this area.

The second fundamental approach explicitly minimizes (or maximizes) the thermodynamic function that defines the equilibrium condition. For many chemical engineering applications this function will be the Gibbs free energy. White *et al.* [65] were the first to solve the problem using optimization techniques. They considered ideal mixtures only and tested two methods, one of which was a steepest descent method while the other relied on techniques of linear programming. It is known as the RAND algorithm. Gautam and Seider [16] used Wolfe's Quadratic Programming Algorithm to compare its performance with the NASA (developed by Gordon and McBride [22]) and RAND algorithms. These two algorithms were shown to be essentially implementations of Newton's method. The approach was extended by Gautam and Seider [18] to handle electrolytic solutions and by White and Seider [64] to solve chemical equilibrium problems where some of the reactions may not be taken at equilibrium. The possibility of convergence to a local solution could not be removed. George *et al.* [19] used an allocation function in conjunction with Powell's [45] method; it gives slower performance than the method of Gautam and Seider [16]. Castillo and Grossmann [10] employ a local optimization approach, the variable-metric projection method, and do not eliminate phases if the mol numbers approach zero. Their approach is extended by Grossmann and Davidson [24] for the case of restricted chemical equilibria. A review of these contributions is given by Seider *et al.* [51].

Soares *et al.* [53] used a Newton-Raphson method to solve the equilibrium problem. The selection of initial conditions is crucial in order to avoid convergence to the trivial solution. Ohanomah and Thompson [40, 41, 42] provide an extensive study on the implementation of the best algorithms available in the literature for the phase equilibrium problem. Both stoichiometric and minimization approaches were tested, and revealed that there are convergence problems for most algorithms when an excess number of phases is assumed. It is interesting to note that the NRTL equation was not used to model the liquid phases because it gave rise to multiple solutions corresponding to potentially false miscibility gaps, highlighting the difficulty associated with its use. Lantagne *et al.* [28] also tested numerous methods including Newton, quasi-Newton, penalty function and SQP methods on a variety of systems including solids and electrolytes. Greiner [23] presented an exact Newton implementation based on the Brinkley-NASA-RAND algorithm that yields rapid quadratic convergence. It requires a good initial guess which is provided by an approach based on linear programming, representing a potential disadvantage in terms of finding the global solution. Lucia and Xu [31] investigated issues of reliability and efficiency for quasi-Newton and Newton methods for several chemical process applications including the calculation of extrema of thermodynamic functions. The importance of good starting points was emphasized, and techniques for their automatic generation were presented.

Gautam and Seider [17] demonstrated how the performance of the RAND algorithm could be considerably improved by using a phase-splitting algorithm in conjunction with it. Guesses for postulated phases in unstable systems were obtained based on activity levels, and the method is relatively insensitive to poor guesses in composition. Walraven and van Rompay [63] presented a modification of the algorithm and reported improved overall performance. Baker *et al.* [1] formalized the concept of phase stability and the tangent plane criterion as first introduced by Gibbs [20, 21] and presented its proof. One advantage of the criterion is that the metastable region is recognized as unstable. The authors point out the pitfalls involved in the prediction of the equilibrium state and how the tangent plane criterion can help in testing if a given phase distribution corresponds to the actual equilibrium state. Michelsen [36, 37] proposed an approach for the implementation of the tangent plane criterion using a variety of computational techniques. Convergence to a local solution is guaranteed, but there is the danger of predicting a stable phase distribution, when, in fact, this is not the case. One advantage of the approach is that if a given phase configuration is unstable then the solutions provide a reasonable guess for initiating the solution search in the new phase space. Nagarajan *et al.* [38, 39] reformulated Michelsen's method in terms of molar densities and reported improvement in the robustness and speed of convergence of the algorithm. Castier *et al.* [9] presented an algorithm that uses a stoichiometric formulation which automatically selects the independent chemical reactions, and Michelsen's [37] approach is used to test for the stability of the obtained phase configurations. Special initialization schemes are necessary to avoid trivial solutions. A review on the issue of phase-splitting is supplied by Swank and Mullins [58], where liquid-liquid problems modeled using the NRTL equation were tested using various combinations of available methods.

An important application of the phase equilibrium problem is that of non-ideal three-phase distillation, of which numerous examples exist in the literature. Block and Hegner [3] were the first to simulate a three phase distillation column and point out the dangers of misguided assumptions on the number of phases that are present. Kovach and Seider [27] presented the first set of experimental data for a three-phase heterogeneous azeotropic distillation column, and traced the temperature front associated with the phase boundary. Cairns and Furzer in a recent series of papers [5, 6, 7] provide extensive results on a 13-component column operating in the three phase region using an algorithm based on Michelsen's approach [36, 37] to predict phase stability throughout the column. The focus of the work is on large-scale distillation simulation. Several thermodynamic models were tested and a thorough review of the three-phase problems tackled in the literature is provided.

Sun and Seider [55] used a Newton-homotopy continuation algorithm to obtain the stationary points of the Gibbs free energy surface. Sun and Seider [56] also apply homotopy techniques to the phase stability problem to generate improved starting points that are used in the search for the global minimum of the Gibbs free energy. This combined approach reduces the risk of failure, but it is not possible to provide a theoretical guarantee that the global solution will be obtained in all cases. The approach has been used successfully to predict the behavior of a difficult three phase azeotropic distillation example.

Paules and Floudas [44] employ the Global Optimal Search algorithm of Floudas *et al.* [12] to find the equilibrium solution. The main feature of this approach is the introduction of binary variables to represent the potential presence or absence of a phase at equilibrium, in an attempt to avoid the difficulties encountered at phase boundaries associated with singularities. Special techniques were used to avoid convergence to metastable points where the Lagrange multipliers become linearly dependent. The approach showed considerable promise but the main drawback is that the Lagrangian functions cannot be guaranteed to provide lower bounds over the complete solution space, so that no claims could be made on whether the obtained solutions were global.

Eubank *et al.* [11] provide an alternative way to predict fluid-phase equilibria, using an area method that integrates the Gibbs energy of mixing curve rather than differentiating it. They cannot guarantee convergence to the true solution if it lies at a composition bound, and the computational effort increases as the square of the desired accuracy. Difficulties arise in extending the approach beyond three components, and a maximum of two phases may be postulated.

It is observed that all the algorithms discussed share one drawback: there is no theoretical guarantee of convergence to the true equilibrium solution – or even to a local minimum of the Gibbs free energy in some cases. Caram and Scriven [8], Othmer [43] and Heidemann [25] show how even simple forms of nonideality can lead to multiple equilibria in closed reacting systems. This represents a serious disadvantage in attempting to describe phase equilibrium where chemical reaction may or may not be occurring. A common problem in liquid-liquid equilibria is convergence to the trivial solution where the mol fractions of all components in both phases are the same, i.e. an incorrect homogeneous solution. Due to the complex and nonlinear nature of the models used to describe the equilibrium situation, there may be several local solutions to the problem at hand. Thus, the certainty of convergence to the global solution for conventional methods will be highly dependent on starting point.

The main contribution of this work is to show that for ideal vapor phases and liquid phases whose behavior may be predicted by the NRTL equation, *attainment of an ϵ-global solution can be guaranteed from any starting point*. Ideal vapor phases are easily incorporated. In terms of extending the approach to nonideal vapor phases, it is possible to use the B–truncated virial equation which provide the fugacity coefficients as bilinear functions of the composition and the GOP algorithm can be used for this class of problems also. Further theoretical and algorithmic developments are needed so as to extend the proposed approach to cubic equations of state, since the fugacities cannot be explicitly calculated in terms of composition.

In the following section, the requisite thermodynamic background for the phase and chemical equilibrium problem is provided, describing the assumptions that are made in this work. Then, a general description of the Global OPtimization algorithm (GOP) of Floudas and Visweswaran [13, 14] is given, outlining the required structure that a problem must possess in order to apply it. The Gibbs free energy expression is analyzed in detail. An important property that simplifies the objective function considerably is introduced. Then, it is described how new transformation variables are introduced so that the problem will possess the structure required by the GOP. For the NRTL equation, the simplifications and transformations of the original formulation yield a biconvex objective function over a nonconvex set of equality constraints. The GOP algorithm can then be employed to theoretically guarantee obtaining the ϵ-global solution. This is an important class of problems for which no previous approach is available that can guarantee attainment of the ϵ-global solution. Examples are presented and they show how convergence to the ϵ-global solution is achieved regardless of the quality of the supplied initial point. The results demonstrate the success of the algorithm in finding equilibrium solutions for a variety of challenging problems.

2 Problem Formulation

In this section, a general outline of the phase and chemical equilibrium problem will be given. Some important assumptions will be discussed along with comments on the range of applicability of the proposed approach. The focus is on systems that attain equilibrium states under conditions of constant temperature and pressure, where the global minimum value of the Gibbs free energy describes the true equilibrium state. This represents the most common approach to the problem, although other thermodynamic criterion can be used (e.g. maximize entropy under adiabatic conditions at constant temperature). The problem may be stated as follows:

> *Given C components participating in up to P potential phases under isothermal and isobaric conditions find the mol vector $\mathbf{n}$ that minimizes the value of the Gibbs free energy while also satisfying the appropriate material balance constraints.*

The set of components is represented by the index set $C = \{i\}$ and the elements that constitute these components are given by $E = \{e\}$. The set of phases is denoted by $P = \{k\}$ where it is composed of vapor and liquid phases, labeled P_V and P_L respectively, so that $P = P_V \cup P_L$. Thus, for a multicomponent, multiphase system, the criterion of equilibrium dictates that the Gibbs free energy function attain its minimum:

$$\min \quad G(\mathbf{n}) \quad = \quad \sum_{i \in C} \sum_{k \in P} n_i^k \mu_i^k$$

$$= \sum_{i \in C} \sum_{k \in P} n_i^k \left\{ \Delta G_i^{k,f} + RT \ln \frac{\hat{f}_i^k}{f_i^{k,0}} \right\} \tag{1}$$

where n_i^k is the number of moles of species i present in phase k, μ_i^k is the associated chemical potential, often expressed through the use of fugacity coefficients described by $\hat{f}_i^k$ for the mixture and $f_i^{k,0}$ for the pure component at the standard state. $\Delta G_i^{k,f}$ represents the Gibbs free energy of formation of component i in phase state k at the system temperature (assuming that the Gibbs energy content of the elemental species at the system temperature is zero).

Difficulties in the use of Eqn. (1) arise due to the complicated expressions available for the expressions for fugacity. The liquid phase is modeled through the use of activity coefficients where the fugacity ratio is expressed as:

$$\frac{f_i^L}{f_i^{L,0}} = \gamma_i^L x_i^L \tag{2}$$

where x_i^L denotes the mole fraction of species i in the liquid phase, and γ_i^L is the corresponding activity coefficient at the system temperature and pressure. If the convention that $\ln \gamma_i \rightarrow 0$ as $x_i \rightarrow 1$ for the activity coefficient is assumed, then the standard state is conveniently taken as the fugacity of the component in its pure state at the temperature and pressure of the system. For low pressure systems, the variance of this quantity with pressure is often not significant.

The fugacity of the vapor phase can be expressed as a function of fugacity coefficients as follows:

$$\frac{f_i^V}{f_i^{V,0}} = \phi_i^V y_i^V P \tag{3}$$

where ϕ_i^V is the partial fugacity coefficient, y_i^V represents the vapor phase mol fraction at a total system pressure P. The standard state for the vapor phase is taken as an ideal gas at unit fugacity at the system temperature where this quantity is usually equal to 1 atm. Occasionally the standard state is given at values of fugacity that differ from one.

Material Balances

The objective function as described by Eqn. (1) must yield a solution that will satisfy the conservation of mass requirements. These can take either of two forms depending on whether reaction occurs in the system and introduce a set of linear equalities into the formulation.

(a) *Elemental Constraints*

For simultaneous phase and chemical equilibrium where reaction does occur, conservation of the constituent atoms must be satisfied:

$$\sum_{i \in C} \sum_{k \in P} a_{ei} n_i^k \quad = b_e \quad \forall \quad e \in E \tag{4}$$

where a_{ei} represents the number of gram-atoms of element e in component i, and b_e the total number of gram-atoms of element e in the system.

(b) *Mass Balance Constraints*

These constraints are required for those systems where no chemical reaction takes place, and thus conservation over the components need only hold:

$$\sum_{k \in P} n_i^k \;=\; n_i^T \quad \forall \quad i \in C \tag{5}$$

where n_i^T is the total number of moles of component i in the beginning mixture.

For notational clarity, the material balance constraints for any system, reacting or non-reacting, will be written in the following general form:

$$\mathbf{A} \cdot \mathbf{n} \;-\; \mathbf{b} = 0 \tag{6}$$

where $\mathbf{n}$ represents the column vector of the component mol numbers, $\mathbf{A}$ is the appropriate elemental or compound abundance matrix, and $\mathbf{b}$ is the column vector of the total amounts of elements or compounds in the system.

Feasibility Constraints

Obviously a physically realizable solution requires that

$$0 \;\leq\; n_i^k \;\leq\; n^T \qquad \forall \; i \in C \;,\; k \in P \tag{7}$$

where n^T is the total number of mols in the system.

Standard State Data:

At this juncture, it is appropriate to discuss assumptions that can be made in regard to the standard state data. If chemical reaction occurs in the system under investigation, then the Gibbs standard free energies of formation are kept as they are in Eqn. (1). For nonreacting systems, it is possible to remove certain constant terms from the objective function under two different scenarios:

Case I: If the system under consideration has no vapor phase postulated, and all the liquid phases share the same standard state, then it is possible to eliminate the Gibbs free energy of formation term due to the following observation:

$$\sum_{i \in C} \sum_{k \in P} n_i^k \Delta G_i^{k,f} \;=\; \sum_{i \in C} \Delta G_i^{L,f} \sum_{k \in P} n_i^k \;=\; \sum_{i \in C} \Delta G_i^{L,f} n_i^T \;=\; \kappa_I \tag{8}$$

where $\Delta G_i^{L,f}$ is the Gibbs formation energy for the liquid phase at the system temperature and pressure and κ_I is a constant. The adjusted objective function, labeled $\hat{G}_I(\mathbf{n})$, now becomes:

$$\min \quad \hat{G}_I(\mathbf{n}) = \sum_{i \in C} \sum_{k \in P} n_i^k \left\{ \frac{\hat{f}_i^k}{f_i^{k,0}} \right\} \equiv \frac{G(\mathbf{n}) - \kappa_I}{RT} \tag{9}$$

where $G(\mathbf{n})$ is defined by Eqn. (1).

Case II: If a vapor phase is present in the system, then the difference between the Gibbs formation energies of the gas and liquid states can usually be adequately approximated by a saturated pressure condensation term as follows:

$$\Delta G_i^{L,f} = \Delta G_i^{V,f} + RT \ln P_i^{SAT} \tag{10}$$

where P_i^{SAT} is the saturated vapor pressure for component i. Stull *et al.* [54] notes that Eqn. (10) is valid for vapor pressures under 2 or 3 atm, but may require the use of fugacity coefficients for systems that associate in the vapor phase. Defining $\kappa_{II} = \sum_i \Delta G_i^{V,f} n_i^T$, the adjusted objective function, labeled $\hat{G}_{II}(\mathbf{n})$, can now be written:

$$\min \quad \hat{G}_{II}(\mathbf{n}) \ = \ \sum_{i \in C} \sum_{k \in P_L} n_i^k \ln P_i^{SAT} + \sum_{i \in C} \sum_{k \in P} n_i^k \left\{ \frac{\hat{f}_i^k}{f_i^{k,0}} \right\} \equiv \frac{G(\mathbf{n}) - \kappa_{II}}{RT} \tag{11}$$

with $G(\mathbf{n})$ given by Eqn. (1). Thus, for phase equilibrium problems when only liquid phases are postulated, Eqns. (9) or (11) can be used to represent the Gibbs free energy function; if a vapor phase is present, then the function to be minimized is given by Eqn. (11). This minimizes the dependence of the reported solutions on the standard Gibbs free energy of formation data.

In conclusion, the complete formulation of the phase and chemical equilibrium for ideal vapor phases and liquid phases whose fugacities can be adequately modeled by the NRTL equation, is given by minimizing the expression of Eqn. (1) subject to the material balance constraints supplied by Eqn. (6) and the feasibility constraints of Eqn. (7). The variables of the formulation are the mol numbers n_i^k. The mol fractions are eliminated by redefining them in terms of the mol numbers as $x_i = n_i / \sum_j n_j \ \forall \ j$ for all phases. There are two important observations in regard to the optimization formulation:

- The constraint set is of small size and linear.
- The only nonlinearity appears in the objective function as $n_i \ln f_i / f_i^0$.

If the system is ideal then any local solution will be the global one. However, the main difficulty is that due to the complex nature of the models used to predict fugacities, highly nonconvex functionalities result. This may lead to local or trivial solutions that are not true equilibrium solutions, and may lie far away from the correct optimal solution. The obtained solution will also be highly dependent on the chosen starting point.

3 Review of the GOP

The requisite background for the global optimization algorithm of Floudas and Visweswaran [13, 14] is now provided. The general form of the optimization problem of interest is given as follows:

$$\left.\begin{array}{rcl} \min\limits_{x,y} \; f(x,y) & & \\ s.t. \quad h(x,y) & = & 0 \\ g(x,y) & \leq & 0 \\ x & \in & X \\ y & \in & Y \end{array}\right\} \tag{12}$$

where X and Y are convex sets, $f(x, y)$ is the objective function to be minimized, and $h(x, y)$ and $g(x, y)$ represent the vectors of equality and inequality constraints respectively. These functions are assumed to be continuous and piecewise differentiable on $X \times Y$. The GOP algorithm can be used to determine an ϵ-global solution for problems that satisfy the following conditions:

Conditions (A):

- $f(x, y)$ and $g(x, y)$ are convex in x for all fixed y and convex in y for all fixed x,
- $h(x, y)$ is affine in x for all fixed y, and affine in y for all fixed x,
- X and Y are nonempty, compact convex sets and a constraint qualification (such as Slater's) is satisfied.

Two key concepts, namely *transformations* and *partitioning*, extend the classes of problems to which the GOP algorithm may be applied. The transformation phase involves the introduction of new variables: this changes the form of the nonconvexities while still maintaining an equivalent formulation. The next step is to partition this new augmented set of variables into two distinct subsets, x and y, such that *Conditions (A)* will be satisfied. Floudas *et al.* [12] present one possible technique for selection of the optimal choice of variable partitions at this step. By making use of these concepts, Floudas and Visweswaran [13, 14] have demonstrated that the GOP algorithm can be applied to general quadratic programming problems, quadratic problems with quadratic constraints, biconvex programming problems with bilinear constraints, polynomial and rational polynomial programming problems. In addition, it has been shown by Liu and Floudas [30] that the GOP can be applied to a large class of general smooth mathematical programming problems (i.e. min $F(x)$ *s.t.* $G(x) \leq 0$) by converting them into the standard form given by (12).

Partitioning the variable set in this way allows the original problem to be decomposed into a simpler subproblem if either one of the variable sets is held constant. The superscript k will correspond to any given iteration of the algorithm in this section. If the y variables are held fixed at the k'th iteration so that $y = y^k$ in (12), then the resulting optimization problem is called the *primal* problem (P). As will be shown in the next section, it is a simple matter to ensure that the primal problem (P) will always be feasible for the phase and chemical equilibrium problem, and therefore the issue of infeasible primal subproblems need not be considered. Note that (P) is a convex subproblem because of *Conditions (A)*, and any feasible local solution to it is a global solution, representing a valid upper bound on the optimal solution of (12).

The next phase is to derive master problems that provide lower bounds on the global solution. By formulating the dual of (12) and successively relaxing it, the *relaxed dual* subproblem is obtained:

$$\begin{aligned} & \min_{\substack{y \in Y \\ \mu_B}} \ \mu_B \\ s.t. \quad \mu_B \ \geq \ & \min_{x \in X} L(x, y, \lambda, \mu) \quad \forall \quad \mu \geq 0 \ , \ \lambda \end{aligned} \tag{13}$$

where $L(x, y, \lambda, \mu) = f(x, y) + \lambda^T h(x, y) + \mu^T g(x, y)$, and is the Lagrangian constructed from problem (12), with λ and μ corresponding to the Lagrange multiplier vectors of its equality and inequality constraints respectively. μ_B is a scalar. The details of the steps in the development of (13) may be found in Floudas and Visweswaran [13, 14]. The inner relaxed dual subproblem at the k'th iteration is defined as:

$$\min_{x \in X} \ L(x, y, \lambda^k, \mu^k) \tag{IRD}$$

where λ^k and μ^k are the vector Lagrange multipliers obtained from the k'th primal problem. Rather than solving this very difficult optimization problem (it is an infinite programming problem in y), the central basis of the GOP algorithm is to replace (IRD) with a set of relaxed dual subproblems that validly underestimate the solution of problem (12). In order to accomplish this, the x and y variables must interact in a bilinear fashion in the Lagrangian defined by (IRD). If the x variables appear in a convex rather than linear form for fixed y, then the Lagrangian is linearized around x^k, the value of x from the k'th primal. For the phase and chemical equilibrium problem, it will be shown in the next section that the interaction between the variables can be made to be purely bilinear, so that this step is not required. This bilinear interaction is required in order that the so called *qualifying constraints*, defined as the derivative of the Lagrange function with respect to the x variables, are functions of the y variables alone. Let $x \equiv \{x_i\}$; then the vector of qualifying constraints from the k'th iteration, labeled $g^k(y)$, is made up of i elements as follows:

$$g^k(y) = \nabla_x L(x, y, \lambda^k, \mu^k) \quad \text{with} \quad g_i^k(y) = \nabla_{x_i} L(x, y, \lambda^k, \mu^k) \tag{14}$$

The set of connected variables, labeled CV, is defined as those variables that interact bilinearly, or equivalently, as those variables for which $g_i^k(y)$ is a function of y. By setting these constraints greater or less than zero, they form hyperplanes that partition the y variable space into subdomains. If N_{CV}^X is the number of x variables, and N_{CV}^Y the number of y variables that interact with each other in a bilinear fashion, then the number of connected variables, N_{CV}, is given as:

$$N_{CV} = \min\{\ N_{CV}^{X}\ ,\ N_{CV}^{Y}\ \} \tag{15}$$

Each $g_i^k(y)$ can be set greater or less than zero, so that there are $2^{N_{CV}}$ ways in which the qualifying constraints can combine to be of constant sign. The quantity $s_i^{B_l} = \pm 1$ is used to decide whether a given qualifying constraint is positive or negative: if $s_i^{B_l} = +1$, then $g_i^k(y) \geq 0$, and if $s_i^{B_l} = -1$, then $g_i^k(y) \leq 0$. B_l represents one combination of qualifying constraints from the set CB, which contains all possible $2^{N_{CV}}$ such combinations. Thus, each B_l has a unique vector $\{s_i^{B_l}\}$ associated with it, whose elements are comprised of ± 1.

If the x variables are constrained as $x_i^L \leq x_i \leq x_i^U \ \forall\ i$, then the linearization of (IRD) shows how the bounds on the x variables can be set on the basis of the sign of the qualifying constraints:

$$\min_{x \in X} L(x, y, \lambda^k, \mu^k) \geq L(x^k, y, \lambda^k, \mu^k) + \min_{x \in X} \sum_{i \in CV} g_i^k(y) \cdot \left[x_i - x_i^k\right] \quad \forall\ y \tag{16}$$

The proof of this lemma follows from the convexity of $L(x, y, \lambda^k, \mu^k)$ for fixed y and is given in Floudas and Visweswaran [13, 14]. If $g_i^k(y)$ is positive, then $x_i - x_i^k$ must be driven to its minimum value if the (IRD) is to be validly underestimated. This is achieved by setting $x_i = x_i^L$, so that the total term $g_i^k(y) \cdot [x_i^L - x_i]$ will go to its minimum. Similarly, if $g_i^k(y)$ is negative, then $x_i - x_i^k$ must be driven to its *maximum* value, which is obtained by setting $x_i = x_i^U$. Then, $g_i^k(y) \cdot [x_i^U - x_i]$ will likewise be driven to its minimum. By replacing the x variables with their bounds in this manner for each possible combination of qualifying constraints, (IRD) is validly underestimated for the complete y variable space. This allows a set of $2^{N_{CV}}$ relaxed dual subproblems to replace (IRD).

Assume that the algorithm has progressed K iterations. Before solving the set of $2^{N_{CV}}$ relaxed dual subproblems, the Lagrangians to be included from previous iterations must be determined by establishing which of the qualifying constraints from the previous iterations are satisfied at the current value of $y = y^K$. For any previous iteration k, the sign of $g^k(y^K)$ decides the bound at which the corresponding x variables should be set, and this combination is denoted $x^{B_j^k}$. If these Lagrangians are included in the formulation, along with the vector of qualifying constraints, $g^k(y)$ for all $k = 1, 2, \ldots, K-1$, then the relaxed dual subproblem for any given combination of bounds B_l from the set CB, is defined as follows:

$$\mu_B^{k_S}(K, B_l) = \left\{ \begin{array}{l} \min\limits_{\substack{y \in Y \\ \mu_B}} \ \mu_B \\ s.t. \\ \left. \begin{array}{lll} \mu_B & \geq & L(x^{B_j^k}, y, \lambda^k, \mu^k) \\ & & g_i^k(y) \geq 0 \ \text{ if } \ g_i^k(y^K) \geq 0 \ \forall\ i \\ & & g_i^k(y) \leq 0 \ \text{ if } \ g_i^k(y^K) \leq 0 \ \forall\ i \end{array} \right\} \ \forall\ k = 1, 2, \ldots, K-1 \\ \begin{array}{lll} \mu_B & \geq & L(x^{B_l}, y, \lambda^K, \mu^K) \\ & & g_i^K(y) \geq 0 \ \text{ if } \ s_i^{B_l} = +1 \ \forall\ i \\ & & g_i^K(y) \leq 0 \ \text{ if } \ s_i^{B_l} = -1 \ \forall\ i \end{array} \end{array} \right\} \text{(RD)}$$

It is convenient to store these solutions at the K'th level of a tree, where this level contains $2^{N_{CV}}$ nodes. Each node k_S is seen to correspond to a subdomain of the y variable space as defined by its qualifying constraints. These nodes are defined over the set (K, CB). The next step is to determine a new lower bound. This is done by choosing the infimum of available lower bounds obtained as solutions from all previous relaxed dual subproblems. The value of y associated with this node supplies y^{K+1} for the next iteration, and the node is then discarded from future consideration.

Thus, the solution procedure dictates that iteration between the primal problem (P) and the set of relaxed dual subproblems of type (RD) until the lower and upper bounds meet within some specified tolerance, ϵ, yields the global solution of (12). A conceptual outline of the GOP algorithm is given in Figure 1. The criteria required to guarantee ϵ-global convergence and optimality are established as follows: if (i) *Conditions (A)* are satisfied, (ii) the set of multipliers of the primal problem is nonempty and bounded, and (iii) $Y \subseteq V$, where $V \equiv \{y : h(x,y) = 0\ ,\ g(x,y) \leq 0 \text{ for some } x\}$, then for any given $\epsilon > 0$, the GOP algorithm terminates in a finite number of steps to an ϵ-global solution of (12). The proof of this can be found in Floudas and Visweswaran [13, 14]. In the following section, it will be demonstrated how the phase and chemical equilibrium problem can be converted into a form that satisfies the required conditions stated above, and how the GOP algorithm is specifically applied to it.

4 Analysis for the NRTL Equation

Renon and Prausnitz [48] derived the following equation for the liquid–phase activity coefficient based on Scott's Two–Liquid theory and using the assumption of Non–Randomness:

$$\ln \gamma_i = \frac{\sum\limits_{j \in C} \tau_{ji} \mathcal{G}_{ji} x_j}{\sum\limits_{j \in C} \mathcal{G}_{ji} x_j} + \sum_{j \in C} \frac{\mathcal{G}_{ij} x_j}{\sum\limits_{l \in C} \mathcal{G}_{lj} x_l} \left\{ \tau_{ij} - \frac{\sum\limits_{l \in C} \tau_{lj} \mathcal{G}_{lj} x_l}{\sum\limits_{l \in C} \mathcal{G}_{lj} x_l} \right\} \qquad \forall\ i \in C \tag{17}$$

where γ_i is the activity coefficient at mol fraction x_i, τ_{ij} are non–symmetric binary interaction parameters, $\mathcal{G}_{ij}$ is a parameter introduced for notational convenience and is based on another adjustable binary parameter α_{ij} (with $\alpha_{ii} = 0$) which does have the property of symmetry ($\alpha_{ij} = \alpha_{ji}$). Then τ_{ij} and $\mathcal{G}_{ij}$ are defined as:

$$\tau_{ij} = \frac{g_{ij} - g_{jj}}{RT} \tag{18}$$

$$\mathcal{G}_{ij} = \exp\left(-\alpha_{ij} \tau_{ij}\right) \tag{19}$$

where g_{ji} is the energy of interaction between the pair $i - j$. Note that τ_{ij} can be negative but $\mathcal{G}_{ij}$ is always positive. One important feature of the NRTL equation is its capability of representing liquid–liquid immiscibility for multicomponent systems with only binary parameters. There are three such parameters for each binary pair.

In this section, the Gibbs free energy expression is analyzed for the case of an ideal vapor phase and liquid phases modeled using the NRTL activity coefficient expression. Eqn. (17) yields exactly the same expression for mol numbers as for mol fractions. Substitution of Eqn. (17) into Eqn. (2) yields the correct liquid phase fugacity term, after rewriting the mol fractions in terms of mol numbers. Eqn. (3) is assumed to define the vapor phase fugacity with $\phi_i^V = 1$. Again, the mol fractions are written in terms of the vapor mol number variables. Substitution of the resultant vapor and liquid phase fugacity equations into Eqn. (1) gives the Gibbs free energy function as follows:

$$\begin{aligned}\min\ \hat{G}(\boldsymbol{n}) \;=\; & \sum_{i\in C}\sum_{k\in P} n_i^k \left\{ \frac{\Delta G_i^{k,f}}{RT} + \ln \frac{n_i^k}{\sum\limits_{j\in C} n_j^k} \right\} \\ & + \sum_{i\in C}\sum_{k\in P_L} n_i^k \left\{ \frac{\sum\limits_{j\in C} \tau_{ji}\mathcal{G}_{ji}n_j^k}{\sum\limits_{j\in C} \mathcal{G}_{ji}n_j^k} + \sum_{j\in C} \frac{\mathcal{G}_{ij}n_j^k}{\sum\limits_{l\in C}\mathcal{G}_{lj}n_l^k} \left\{ \tau_{ij} - \frac{\sum\limits_{l\in C}\tau_{lj}\mathcal{G}_{lj}n_l^k}{\sum\limits_{l\in C}\mathcal{G}_{lj}n_l^k} \right\} \right\}\end{aligned} \tag{20}$$

where $\hat{G}(\boldsymbol{n}) = G(\boldsymbol{n})/RT$ (i.e. dimensionless G). Note that the pressure term associated with the fugacity of the vapor phase has been incorporated into the Gibbs energy of formation term, i.e. $\Delta G_i^{V,f} = \Delta G_i^{V,f} + RT \ln P$. This is done in order to collect the linear terms of the objective function.

4.1 Analysis of Gibbs free energy function:

It would appear that $\hat{G}(\boldsymbol{n})$ is a complex, highly nonconvex expression. However, the situation is considerably improved by the following property:

Property 4.1 *For each phase $k \in P$, the following relation is true:*

$$\sum_{i\in C} n_i^k \left\{ \frac{\sum\limits_{j\in C} \tau_{ji}\mathcal{G}_{ji}n_j^k}{\sum\limits_{j\in C} \mathcal{G}_{ji}n_j^k} \right\} - \sum_{i\in C} n_i^k \left\{ \sum_{j\in C} \frac{\mathcal{G}_{ij}n_j^k}{\sum\limits_{l\in C}\mathcal{G}_{lj}n_l^k} \frac{\sum\limits_{l\in C}\tau_{lj}\mathcal{G}_{lj}n_l^k}{\sum\limits_{l\in C}\mathcal{G}_{lj}n_l^k} \right\} = 0 \tag{21}$$

Proof: See McDonald and Floudas [33].

Illustration: An illustration for the two component case, i.e. $\{i_1, i_2\} \in C$, is now provided to demonstrate the usefulness of Property 4.1. The phase superscript k is dropped for clarity of presentation. In what follows, it is seen that instead of summing across the rows, the columns are traversed extracting the common term $\sum_j \mathcal{G}_{ji}n_j$. In addition, the mol number variable to the immediate right of the minus sign in Eqn. (21) is swapped with the first mol number variable of the numerator of the postmultiplying term in braces.

$$\begin{aligned}& \sum_{i\in C} n_i \left\{ \frac{\sum\limits_{j\in C} \tau_{ji}\mathcal{G}_{ji}n_j}{\sum\limits_{j\in C} \mathcal{G}_{ji}n_j} \right\} - \sum_{i\in C} n_i \left\{ \sum_{j\in C} \frac{\mathcal{G}_{ij}n_j}{\sum\limits_{l\in C}\mathcal{G}_{lj}n_l} \frac{\sum\limits_{l\in C}\tau_{lj}\mathcal{G}_{lj}n_l}{\sum\limits_{l\in C}\mathcal{G}_{lj}n_l} \right\} \\ = \;& n_1 \left[\frac{\tau_{21}\mathcal{G}_{21}n_2}{n_1 + \mathcal{G}_{21}n_2} \right] + n_2 \left[\frac{\tau_{12}\mathcal{G}_{12}n_2}{\mathcal{G}_{12}n_1 + n_2} \right]\end{aligned}$$

$$
\begin{aligned}
&- \quad n_1 \left[\frac{n_1}{(n_1+\mathcal{G}_{21}n_2)}\frac{\tau_{21}\mathcal{G}_{21}n_2}{(n_1+\mathcal{G}_{21}n_2)}\right] - n_1 \left[\frac{\mathcal{G}_{12}n_2}{(\mathcal{G}_{12}n_1+n_2)}\frac{\tau_{12}\mathcal{G}_{12}n_1}{(\mathcal{G}_{12}n_1+n_2)}\right] \\
&- \quad n_2 \left[\frac{\mathcal{G}_{21}n_1}{(n_1+\mathcal{G}_{21}n_2)}\frac{\tau_{21}\mathcal{G}_{21}n_2}{(n_1+\mathcal{G}_{21}n_2)}\right] - n_2 \left[\frac{n_2}{(\mathcal{G}_{12}n_1+n_2)}\frac{\tau_{12}\mathcal{G}_{12}n_1}{(\mathcal{G}_{12}n_1+n_2)}\right] \\
&= \quad \frac{1}{n_1+\mathcal{G}_{21}n_2}\cdot n_1 \cdot \left\{\tau_{21}\mathcal{G}_{21}n_2 - n_1\cdot\frac{\tau_{21}\mathcal{G}_{21}n_2}{n_1+\mathcal{G}_{21}n_2} - \mathcal{G}_{21}n_2\cdot\frac{\tau_{21}\mathcal{G}_{21}n_2}{n_1+\mathcal{G}_{21}n_2}\right\} \\
&+ \quad \frac{1}{\mathcal{G}_{12}n_1+n_2}\cdot n_2 \cdot \left\{\tau_{12}\mathcal{G}_{12}n_2 - \mathcal{G}_{12}n_1\cdot\frac{\tau_{12}\mathcal{G}_{12}n_1}{\mathcal{G}_{12}n_1+n_2} - n_2\cdot\frac{\tau_{12}\mathcal{G}_{12}n_1}{\mathcal{G}_{12}n_1+n_2}\right\} \\
&= \quad \frac{1}{n_1+\mathcal{G}_{21}n_2}\cdot n_1\cdot\tau_{21}\mathcal{G}_{21}n_2\cdot\left\{1-\frac{n_1+\mathcal{G}_{21}n_2}{n_1+\mathcal{G}_{21}n_2}\right\} \\
&+ \quad \frac{1}{\mathcal{G}_{12}n_1+n_2}\cdot n_2\cdot\tau_{12}\mathcal{G}_{12}n_2\cdot\left\{1-\frac{\mathcal{G}_{12}n_1+n_2}{\mathcal{G}_{12}n_1+n_2}\right\} \\
&= \quad 0
\end{aligned}
$$

This property reduces the complexity of Eqn. (20) greatly, and it brings the advantage of having bilinear, rather than trilinear, fractional functions in the expression for the objective function. □

Property 4.2 *If $\mathcal{C}^k$ is defined as follows:*

$$
\mathcal{C}^k = \sum_{i\in C} n_i^k \left\{ \frac{\Delta G_i^{k,f}}{RT} + \ln \frac{n_i^k}{\sum\limits_{j\in C} n_j^k} \right\} \qquad \forall\, k \in P \tag{22}
$$

then the quantity $\sum\limits_k \mathcal{C}^k$ is convex.

Proof: The quantity $\mathcal{C}^k$ corresponds to the ideal Gibbs free energy for any given phase k, and its convexity is a well established property (for example, see White *et al.* [65]). A summation of these convex terms over the set of k phases will obviously be convex. □

This means that the objective function can now be written as a combination of a convex portion, and a nonconvex portion:

$$
\min\ \hat{G}(\boldsymbol{n}) \ = \ \sum_{k\in P}\mathcal{C}^k + \sum_{i\in C}\sum_{k\in P_L} n_i^k \left\{ \sum_{j\in C} \frac{\mathcal{G}_{ij}\tau_{ij}n_j^k}{\sum\limits_{l\in C}\mathcal{G}_{lj}n_l^k} \right\} \tag{23}
$$

The nonconvexities now lie solely in the term to the right of the plus sign. The following NonConvex Formulation (NCF) is a new formulation:

$$
\left.
\begin{aligned}
\min \quad & \hat{G}(\boldsymbol{n}) \\
s.t. \quad & \mathbf{A}\cdot\mathbf{n} \ - \ \mathbf{b} = \mathbf{0} \\
& \mathbf{0} \ \le \ \mathbf{n} \ \le \ n^T
\end{aligned}
\right\} \text{(NCF)}
$$

where $\hat{G}(\boldsymbol{n})$ is defined by Eqn. (23) and is a much simpler form for the Gibbs free energy function than that given by Eqn. (20).

4.2 Transformations and Partitioning

It is now convenient to introduce new variables in order to change the nature of the nonconvexities in the objective function. Having augmented the variable set in this way, it is then partitioned into two variable subsets, so that *Conditions (A)* of the GOP are satisfied. If the following new variables are introduced:

$$\Psi_i^k = \frac{n_i^k}{\sum\limits_{j \in C} \mathcal{G}_{ji} n_j^k} \qquad \forall \; i \in C \; , \; k \in P_L \tag{24}$$

then the transformed objective function becomes:

$$\min \; \hat{G}(\boldsymbol{\Psi}, \boldsymbol{n}) = \sum_{k \in P} \mathcal{C}^k + \sum_{i \in C} \sum_{k \in P_L} n_i^k \left\{ \sum_{j \in C} \mathcal{G}_{ij} \tau_{ij} \Psi_j^k \right\} \tag{25}$$

This is now subject to the transformation constraint Eqn. (24) in addition to the material balance constraints as defined by Eqn. (6). Eqn. (24) is reformulated so that this constraint will be of bilinear form as follows:

$$\Psi_i^k \cdot \left\{ \sum_{j \in C} \mathcal{G}_{ji} n_j^k \right\} = n_i^k \qquad \forall \; i \in C \; , \; k \in P_L \tag{26}$$

The objective is to partition the variable set into two subsets so that if either of these subsets is held constant, an optimization problem with simpler structure remains. An examination of Eqn. (25) leads to the conclusion that the obvious partition of variables is that in which the y variable set contains the mol vector, with the x variable set containing the new transforming variables:

$$y \leftarrow \left\{ n_i^k \right\} \equiv \boldsymbol{n} \qquad x \leftarrow \left\{ \Psi_i^k \right\} \equiv \boldsymbol{\Psi} \tag{27}$$

Notice that if the mol number variable set is held constant, a linear objective function results. On the other hand, if the transformed variable set is held constant, a convex objective function is obtained. The equality constraints are of bilinear form and so will yield linear terms if either of the subsets is held constant. It should be noted that the material balance equations depend on the mol numbers alone, and therefore have no interaction with the x variable set. Thus, *Conditions (A)* of the GOP are satisfied. The form of the nonconvexities of the objective function have been changed, and the price paid for obtaining this structure is that additional *bilinear* constraints have been introduced into the system.

4.3 The Primal Problem

The primal problem is defined as the subproblem that results when the y variable set is held fixed. In what follows, overbars on variables represent the values that are held fixed during solution of any given primal problem, which is defined as follows:

$$\left.\begin{aligned}\min \quad \hat{G}(\boldsymbol{\Psi},\bar{\boldsymbol{n}}) &\equiv \sum_{k\in P}\bar{\mathcal{C}}^k + \sum_{i\in C}\sum_{k\in P_L} \bar{n}_i^k \left\{\sum_{j\in C}\mathcal{G}_{ij}\tau_{ij}\Psi_j^k\right\} \\ s.t. \quad \Psi_i^k\cdot\left\{\sum_{j\in C}\mathcal{G}_{ji}\bar{n}_j^k\right\} &= \bar{n}_i^k \qquad \forall\ i\in C\ ,\ k\in P_L\end{aligned}\right\} \qquad \text{(P)}$$

$\bar{\boldsymbol{n}}$ represents the current value of the mol numbers (the y variable set). The primal problem (P) is always feasible provided that the mol vector satisfies the material balance constraints which are functions of the y variables alone. Hence they can be carried directly to the relaxed dual subproblems. This is the reason the material balance constraints are not included in (P). Notice that (P) is merely a function evaluation as the x variable set is completely specified by $\bar{\boldsymbol{n}}$ through the set of equality constraints of (P).

It will be necessary to use the Karush-Kuhn-Tucker (KKT) conditions for the primal problem in proceeding sections. The Lagrangian as constructed from the primal problem for fixed $\bar{\boldsymbol{n}}$ is given as:

$$\begin{aligned}L(\boldsymbol{\Psi},\bar{\boldsymbol{n}},\boldsymbol{\lambda}) &= \sum_{k\in P}\bar{\mathcal{C}}^k + \sum_{i\in C}\sum_{k\in P_L}\bar{n}_i^k\left\{\sum_{j\in C}\mathcal{G}_{ij}\tau_{ij}\Psi_j^k\right\} \\ &+ \sum_{i\in C}\sum_{k\in P_L}\lambda_{\Psi_i^k}\left\{\Psi_i^k\cdot\sum_{j\in C}\mathcal{G}_{ji}\bar{n}_j^k - \bar{n}_i^k\right\}\end{aligned} \qquad (28)$$

where $\lambda_{\Psi_i^k}$ is the multiplier associated with the corresponding constraint that defines the x variable Ψ_i^k. The evaluation of the KKT conditions for the primal yields:

$$\nabla_{\Psi_i^k}L(\boldsymbol{\Psi},\bar{\boldsymbol{n}},\boldsymbol{\lambda}) = \sum_{j\in C}\mathcal{G}_{ji}\tau_{ji}\bar{n}_j^k + \lambda_{\Psi_i^k}\cdot\sum_{j\in C}\mathcal{G}_{ji}\bar{n}_j^k = 0 \qquad \forall\, i\ \in C\ ,\ k\ \in P_L \qquad (29)$$

The Lagrange multipliers from the primal are then explicitly calculated as:

$$\lambda_{\Psi_i^k} = -\frac{\sum_{j\in C}\mathcal{G}_{ji}\tau_{ji}\bar{n}_j^k}{\sum_{j\in C}\mathcal{G}_{ji}\bar{n}_j^k} \qquad \forall\, i\ \in C\ ,\ k\ \in P_L \qquad (30)$$

If a given phase k disappears so that $n_i^k = 0\ \forall\ i$, then the denominator of Eqn. (30) approaches 0. In this case, $\lambda_{\Psi_i^k} = 0\ \forall\ i$ for the phase k will ensure that the KKT conditions of the primal problem are satisfied, as the corresponding constraints of the primal are $\Psi_i^k\ \cdot\ 0 = 0\ \forall\, i$. This eliminates the problem of obtaining unbounded Lagrange multipliers. Thus, the multipliers from any primal problem are nonempty and bounded for all $y\in Y$, a required condition to guarantee ϵ-global convergence. Clearly, the evaluation of the primal problem and the corresponding multipliers amounts to simple function evaluations.

4.4 The Relaxed Dual problem

The primal problem establishes upper bounds on the solution. The relaxed dual subproblems supply lower bounds on the global solution. Their basic structure has been described in Section 3. Because the derivation of the Lagrangian is somewhat involved, it will be illustrated throughout the development for the simple case of a binary system consisting of a single liquid phase. The Lagrange function for this simple example is now given.

Illustration: There are two components and one phase, so that n_1 and n_2 represent the variables of the problem. If the linear terms are neglected, then the convex portion $\mathcal{C}$ of the Gibbs free energy is defined by Eqn. (22) as:

$$\mathcal{C} = n_1 \ln \frac{n_1}{n_1 + n_2} + n_2 \ln \frac{n_2}{n_1 + n_2}$$

The Lagrange function can then be written as:

$$\begin{aligned} L^1(\boldsymbol{\Psi}, \boldsymbol{n}, \boldsymbol{\lambda}) &= \mathcal{C} + n_1 \Psi_2 \cdot \mathcal{G}_{12} \tau_{12} + n_2 \Psi_1 \cdot \mathcal{G}_{21} \tau_{21} \\ &+ \lambda_1 \cdot \{ \Psi_1 [\, n_1 + \mathcal{G}_{21} n_2 \,] - n_1 \} + \lambda_2 \cdot \{ \Psi_2 [\, \mathcal{G}_{12} n_1 + n_2 \,] - n_2 \} \end{aligned}$$

The derivatives of this Lagrange function with respect to the x variables will be required, and for fixed $\boldsymbol{n} = \bar{\boldsymbol{n}}$, they are given as:

$$\begin{aligned} \nabla_{\Psi_1} L(\boldsymbol{\Psi}, \bar{\boldsymbol{n}}, \boldsymbol{\lambda}) &= \bar{n}_2 \cdot \mathcal{G}_{12} \tau_{12} + \lambda_1 \cdot [\, \bar{n}_1 + \mathcal{G}_{21} \bar{n}_2 \,] \\ \nabla_{\Psi_2} L(\boldsymbol{\Psi}, \bar{\boldsymbol{n}}, \boldsymbol{\lambda}) &= \bar{n}_1 \cdot \mathcal{G}_{21} \tau_{21} + \bar{\lambda}_2 \cdot [\, \mathcal{G}_{12} \bar{n}_2 + \bar{n}_2 \,] \end{aligned}$$

It will now be shown how this Lagrange function can be manipulated so as to replace the (IRD) problem defined in Section 3. □

4.4.1 Derivation of the Lagrangian

The first step in deriving the Lagrangian is to separate and collect all the x variable terms so their interaction with the y variable set can be examined. For any fixed $\boldsymbol{\lambda} = \bar{\boldsymbol{\lambda}}$:

$$L(\boldsymbol{\Psi}, \boldsymbol{n}, \bar{\boldsymbol{\lambda}}) = \sum_{i \in C} \sum_{k \in P_L} \Psi_i^k \left\{ \sum_{j \in C} \mathcal{G}_{ji} \tau_{ji} n_j^k + \bar{\lambda}_{\Psi_i^k} \cdot \sum_{j \in C} \mathcal{G}_{ji} n_j^k \right\} + \sum_{k \in P} \mathcal{C}^k - \sum_{i \in C} \sum_{k \in P_L} n_i^k \bar{\lambda}_{\Psi_i^k} \tag{31}$$

This corresponds to the Lagrange function of the (IRD) of Section 3. It differs from the one of Eqn. (28) in that it is written for any y. By subtracting Eqn. Set (29) written for $\boldsymbol{\lambda} = \bar{\boldsymbol{\lambda}}$ from the terms within the curly braces of Eqn. (31) and collecting the terms in n_i^k together, the following expression is obtained:

$$L(\boldsymbol{\Psi}, \boldsymbol{n}, \bar{\boldsymbol{\lambda}}) = \sum_{i \in C} \sum_{k \in P_L} \Psi_i^k \left\{ \sum_{j \in C} \mathcal{G}_{ji} \left[\tau_{ji} + \bar{\lambda}_{\Psi_i^k} \right] \left[n_j^k - \bar{n}_j^k \right] \right\} + \sum_{k \in P} \mathcal{C}^k - \sum_{i \in C} \sum_{k \in P_L} n_i^k \bar{\lambda}_{\Psi_i^k} \tag{32}$$

Evaluating the gradients of the Lagrangian given by Eqn. (32) with respect to the x variables gives:

$$g_i^k(y) = \nabla_{\Psi_i^k} L(\boldsymbol{\Psi}, \boldsymbol{n}, \bar{\boldsymbol{\lambda}}) = \sum_{j \in C} \mathcal{G}_{ji} \left[\tau_{ji} + \bar{\lambda}_{\Psi_i^k}\right] \cdot \left[n_j^k - \bar{n}_j^k\right] \qquad \forall\, i \in C \;,\; k \in P_L \tag{33}$$

These are the *qualifying constraints* written in terms of the y variables and describe the fundamental nature of the interaction of the two variable subsets. Notice that each x variable multiplies a *summation* of y variables in Eqn. (33), so that these constraints form hyperplanes that partition the y variable space.

Illustration – *continued*: Collecting the x variables of $L^1(\boldsymbol{\Psi}, \boldsymbol{n}, \bar{\boldsymbol{\lambda}})$ yields:

$$\begin{aligned} L^2(\boldsymbol{\Psi}, \boldsymbol{n}, \bar{\boldsymbol{\lambda}}) &= C - n_1\bar{\lambda}_1 - n_2\bar{\lambda}_2 \\ &+ \quad \Psi_1 \cdot \{n_2\mathcal{G}_{21}\tau_{21} + \bar{\lambda}_1\,[\,n_1 + \mathcal{G}_{21}n_2\,]\} + \Psi_2 \cdot \{n_1\mathcal{G}_{12}\tau_{12} + \bar{\lambda}_2\,[\,\mathcal{G}_{21}n_1 + n_2\,]\} \end{aligned}$$

For any given primal problem, the KKT conditions yield $\nabla_{\Psi_i} L(\boldsymbol{\Psi}, \bar{\boldsymbol{n}}, \boldsymbol{\lambda}) = 0 \; \forall\, i$ and are clearly satisfied for $\boldsymbol{\lambda} = \bar{\boldsymbol{\lambda}}$. Subtracting these derivatives from the terms within the curly braces of $L^2(\boldsymbol{\Psi}, \boldsymbol{n}, \bar{\boldsymbol{\lambda}})$ allows the terms multiplying the x variables to be written in the form $n_i^k - \bar{n}_i^k$. After collecting the terms in n_i together, the following result is obtained:

$$\begin{aligned} L^3(\boldsymbol{\Psi}, \boldsymbol{n}, \bar{\boldsymbol{\lambda}}) &= C - n_1\bar{\lambda}_1 - n_2\bar{\lambda}_2 \\ &+ \quad \Psi_1 \cdot \{\bar{\lambda}_1\,[\,n_1 - \bar{n}_1\,] + \mathcal{G}_{21}\,[\,\tau_{21} + \bar{\lambda}_1\,]\,[\,n_2 - \bar{n}_2\,]\} \\ &+ \quad \Psi_2 \cdot \{\mathcal{G}_{12}\,[\,\tau_{12} + \bar{\lambda}_2\,]\,[\,n_1 - \bar{n}_1\,] + \bar{\lambda}_2\,[\,n_2 - \bar{n}_2\,]\} \end{aligned}$$

The qualifying constraints are then defined as:

$$\begin{aligned} \nabla_{\Psi_1} L(\boldsymbol{\Psi}, \boldsymbol{n}, \bar{\boldsymbol{\lambda}}) &= \bar{\lambda}_1\,[\,n_1 - \bar{n}_1\,] + \mathcal{G}_{21}\,[\,\tau_{21} + \bar{\lambda}_1\,]\,[\,n_2 - \bar{n}_2\,] \\ \nabla_{\Psi_2} L(\boldsymbol{\Psi}, \boldsymbol{n}, \bar{\boldsymbol{\lambda}}) &= \mathcal{G}_{12}\,[\,\tau_{12} + \bar{\lambda}_2\,]\,[\,n_1 - \bar{n}_1\,] + \bar{\lambda}_2\,[\,n_2 - \bar{n}_2\,] \end{aligned}$$

The form of these constraints will be changed in the following. □

The next important step in the development is to obtain a much simpler set of partitioning hyperplanes. This is achieved by simply augmenting the set of x variables, so that each one of these new x variables will interact with a *single* y variable, rather than a summation of them. This augmented set of variables, denoted $\{\hat{\Psi}_{ij}^k\}$, is defined for each $\{i, k\} \in C \times P_L$ as follows:

$$\hat{\Psi}_{ij}^k = \Psi_i^k \qquad \forall\, j \in C \tag{34}$$

The x variables are now allowed to appear within the innermost summation of Eqn. (32) to yield an equivalent Lagrangian defined as follows:

$$
\begin{aligned}
L(\hat{\boldsymbol{\Psi}}, \boldsymbol{n}, \bar{\boldsymbol{\lambda}}) &= \sum_{i\in C}\sum_{k\in P_L}\left\{\sum_{j\in C}\hat{\Psi}_{ij}^{k}\left[\mathcal{G}_{ji}\left\{\tau_{ji}+\bar{\lambda}_{\Psi_i^k}\right\}\right]\cdot\left[n_j^k-\bar{n}_j^k\right]\right\} \\
&+ \sum_{k\in P}\mathcal{C}^k+\sum_{i\in C}\sum_{k\in P_L} n_i^k\left\{\sum_{j\in C}\mathcal{G}_{ij}\tau_{ij}\bar{\Psi}_j^k\right\}
\end{aligned}
\tag{35}
$$

Eqn. Set (30) has been used to modify the terms involving $\bar{\lambda}_{\Psi_i^k}$ to the right of the minus sign of Eqn. (32). This has been done solely to demonstrate that if $\boldsymbol{n}=\bar{\boldsymbol{n}}$, then the Lagrangian equals the objective function value supplied by the primal at $\bar{\boldsymbol{n}}$. This is a statement of strong duality theory. Eqn. (35) now supplies the new form of the qualifying constraints, labeled $\hat{g}_{ij}^k(y)$, obtained from the modified Lagrangian of Eqn. (35) as:

$$
\hat{g}_{ij}^k(y)=\nabla_{\hat{\Psi}_{ij}^k}L(x,y,\bar{\lambda})=\mathcal{G}_{ji}\left[\tau_{ji}+\bar{\lambda}_{\Psi_i^k}\right]\cdot\left[n_j^k-\bar{n}_j^k\right]\quad\forall\, i\in C\ ,\ j\in C\ ,\ k\in P_L \tag{36}
$$

Thus, each qualifying constraint is now a function of a single y variable, with the important result that the partitioning hyperplanes are now orthogonal to each other, and partition the y variable space into n-rectangles (i.e. simple boxes). The number of connected variables is given as:

$$
\begin{aligned}
N_{CV} &= \min\left\{\ N_{CV}^X\ ,\ N_{CV}^Y\ \right\} \\
&= \min\left\{\ |C|^2\cdot|P_L|\ ,\ |C|\cdot|P_L|\ \right\} \\
&= |C|\cdot|P_L|
\end{aligned}
$$

where the braces signify the cardinalities of the appropriate sets. Therefore, it is evident that augmenting the set of x variables in such a way does *not* increase the number of connected variables.

The key point to note about Eqn. (36) is that each qualifying constraint shares the same basic form, defined as $(n_j^k-\bar{n}_j^k)$. The only difference is the expression that premultiplies this term. These are constants that depend on the parameters of the NRTL model and information from the primal in the form of the Lagrange multipliers. Eqn. (7) delineates the feasible region as an n-rectangle. The initial *parent* region is described by this n-rectangle, and its bounds are represented by $R\{\mathcal{L}^R,\mathcal{U}^R\}$, where $\mathcal{L}^R=\{\mathcal{L}^R_{n_i^k}\}$ and $\mathcal{U}^R=\{\mathcal{U}^R_{n_i^k}\}$ comprise the regional bounds for the variables $\{n_i^k\}$. Upon choosing an initial point $\{\bar{n}_i^k\}$, this parent n-rectangle is partitioned by N_{CV} orthogonal hyperplanes passing through $\{\bar{n}_i^k\}$, so that $2^{N_{CV}}$ new n-rectangles are created. Within each of these new n-rectangles, the sign of $(n_i^k-\bar{n}_i^k)$ will be constant $\forall\ \ i\in C\ ,\ k\in P_L$. The bounds for each of these n-rectangles are described as the *box* bounds, denoted $B\{\mathcal{L}^B,\mathcal{U}^B\}$, with $\mathcal{L}^B=\{\mathcal{L}^B_{n_i^k}\}$ and $\mathcal{L}^B=\{\mathcal{U}^B_{n_i^k}\}$ representing the individual box bounds for the variables $\{n_i^k\}$. The set of all possible combinations of box bounds is denoted by CB, with its $2^{N_{CV}}$ members individually referred to as B_l. The parameter $s_{ik}^{B_l}$ is used to delineate each of these box regions and is defined over $C\times P_L\times CB$.

It determines the partition of the y variable space for any given B_l as follows:

$$\left.\begin{array}{llll} \text{If} & s_{ik}^{B_l} = +1 & \text{then} & n_i^k - \bar{n}_i^k \geq 0 \\ \text{If} & s_{ik}^{B_l} = -1 & \text{then} & n_i^k - \bar{n}_i^k < 0 \end{array}\right\} \quad \forall\, i \in C \,,\, k \in P_L$$

Figure 2 shows how $s_{ik}^{B_l}$ is used to create these regional and box bounds at the first iteration for the case of 2 connected variables, with $C \equiv \{i_1, i_2\}$ and $P_L \equiv \{k_1\}$. The initial point generates 4 subdomains denoted B_1 through B_4.

This implies that it is possible to construct Lagrangians that validly underestimate the global solution in each of these n-rectangles, within which an individual relaxed dual subproblem is solved. If the solution is greater than the current best upper bound obtained from the primal problem, it may be fathomed (i.e. discarded); otherwise, it is added to the set of candidate lower bounds. The infimum of all such solutions supplies the point for the next iteration, where this single n-rectangle will again be partitioned into $2^{N_{CV}}$ n-rectangles to supply additional lower bounds on the final solution. In the context of Figure 2, suppose the infimum of the 4 lower bounds lies in B_2. At the next iteration, B_2 is divided into 4 regions, and so on.

A convenient way of describing this partitioning of the y variable space in the branch and bound approach is through the use of a tree structure. The starting point is represented by the *root* node, labeled R, and it generates $2^{N_{CV}}$ nodes at the first level of the tree. One of these leaf nodes becomes the next iteration node, in turn generating a further $2^{N_{CV}}$ additional nodes, and so on. This is illustrated in Figure 3 for two connected variables where the nodes for the first three iterations are numbered 1 through 12. Note that a maximum of 2^2 nodes are generated at each iteration and that at any given iteration K, all generated solution nodes share the same parent node. Such a structure has certain advantageous features, namely:

(i) The qualifying constraints are a *single* set of box bounds on the variables, rather than sets of constraints generated from current and previous iterations.

(ii) Each n-rectangle is a refinement of its parent n-rectangle so that the regional bounds for a given node are supplied by the box bounds of its parent node. This has the important implication that any given Lagrangian will be valid in any future n-rectangles that it spawns.

(iii) Because of (ii), retrieving previous Lagrangians, labeled K_P, for use in the current relaxed dual subproblem is especially simple. A backward depth-first traversal through the solution tree from the current node to the root node, extracting the relevant information required to construct the Lagrangian at each node along the path, generates the set of valid Lagrangians, denoted $PL(K_P)$. This set of Lagrange functions is included in *each* relaxed dual subproblem.

Point (iii) above brings the extremely important computational advantage that each relaxed dual subproblem contains relatively few Lagrangians from previous iterations. This is because a Lagrangian is not included for *all* previous iterations, but only for those whose nodes define the current node as a subdomain in the y variable space. This is shown in Figure 3 where only one Lagrangian from previous iterations is used at both the second *and* third iteration. Thus, each relaxed dual subproblem can be both generated and solved efficiently. The manner in which the x variable bounds are obtained and set on the basis of the qualifying constraints will now be described.

4.4.2 Evaluating x variable bounds

It is necessary to establish upper and lower bounds on the x variables within any given n-rectangle defined by $B\{\mathcal{L}^B, \mathcal{U}^B\}$. Recall that $\{\Psi_i^k\}$ are defined as linear fractionals. Any linear fractional is a pseudolinear function, that is, it is pseudoconvex *and* pseudoconcave. Thus, there is one local minimum and one local maximum that satisfy the KKT optimality conditions, and these will be unique global extrema. By examining the KKT conditions $\forall\ i \in C$, $\forall\ k \in P_L$ for the following problem:

$$\min \quad \Psi_i^k \quad s.t. \quad \mathcal{L}^B_{n_j^k} \leq n_j^k \leq \mathcal{U}^B_{n_j^k} \qquad \forall\, j \in C \tag{37}$$

the global minimum value for each Ψ_i^k in $B\{\mathcal{L}^B, \mathcal{U}^B\}$ can be evaluated and is labeled $\mathcal{L}_{\Psi_i^k}$. $-\Psi_i^k$ is minimized subject to the same constraints to obtain the corresponding maximum, $\mathcal{U}_{\Psi_i^k}$. Appendix A shows that the globally valid lower and upper bounds for Ψ_i^k (and hence $\hat{\Psi}_{ij}^k$) within the n-rectangle defined by $B\{\mathcal{L}^B, \mathcal{U}^B\}$ are given as:

$$\mathcal{L}_{\Psi_i^k} = \frac{\mathcal{L}^B_{n_i^k}}{\mathcal{L}^B_{n_i^k} + \sum\limits_{j \neq i} \mathcal{G}_{ji}\, \mathcal{U}^B_{n_j^k}} \qquad \text{and} \qquad \mathcal{U}_{\Psi_i^k} = \frac{\mathcal{U}^B_{n_i^k}}{\mathcal{U}^B_{n_i^k} + \sum\limits_{j \neq i} \mathcal{G}_{ji}\, \mathcal{L}^B_{n_j^k}} \tag{38}$$

4.4.3 Setting the bounds on the x variables

The final expression for the Lagrange function collects the terms in n to yield:

$$L(\hat{\Psi}, n, \bar{\lambda}) = \sum_{i \in C} \sum_{k \in P_L} \left\{ \left[\, n_i^k - \bar{n}_i^k \,\right] \cdot \sum_{j \in C} \hat{\Psi}_{ji}^k \left[\, \mathcal{G}_{ij} \left\{ \tau_{ij} + \bar{\lambda}_{\Psi_i^k} \right\} \right] \right\} + \sum_{k \in P} \mathcal{C}^k - \sum_{i \in C} \sum_{k \in P_L} n_i^k \bar{\lambda}_{\Psi_i^k} \tag{39}$$

For some $B_l \in CB$, it is required to set the bounds on $\hat{\Psi}_{ji}^k$ for the current iteration, K, and the set of previous iterations, K_P. Two quantities decide whether the x variables are set at their lower or upper bounds. The first of these is the sign of the term $n_i^k - \bar{n}_i^k$ for current and previous iterations, and the second is the parameter $\bar{s}_{ji}^k$, used to determine the sign of the term that post–multiplies the x variables in Eqn. (39) as follows:

$$\bar{s}_{ji}^k = \begin{cases} +1 & \text{if} \quad \mathcal{G}_{ij} \left[\, \tau_{ij} + \bar{\lambda}_{\Psi_i^k} \,\right] \geq 0 \\ -1 & \text{otherwise} \end{cases}$$

If the combined sign of these terms is positive, then the x variable is set to its *lower* bound, and if it is negative, then the x variable is set to its *upper* bound so that the corresponding terms in the Lagrange functions are validly underestimated. For the current iteration, K, $s_{ik}^{B_l}$ clearly determines the sign of $n_i^k - \bar{n}_i^k$, while for for the set of previous iterations, $PL(K_P)$, the sign of the quantity

$(\bar{n}_i^k)^K - (\bar{n}_i^k)^{K_P}$ properly determines the sign of $n_i^k - (\bar{n}_i^k)^{K_P}$ in the current region. In summary, the following set of steps performed for each $\{i, j, k\} \in C \times C \times P_L$ provide the correct bounds on the x variables:

Current Iteration, K:

$$\text{If} \quad (\bar{s}_{ji}^k)^K \cdot s_{ik}^{B_l} = +1 \quad \text{then} \quad (\hat{\Psi}_{ji}^k)^{B_l^K} = \mathcal{L}_{\Psi_j^k}$$
$$\text{If} \quad (\bar{s}_{ji}^k)^K \cdot s_{ik}^{B_l} = -1 \quad \text{then} \quad (\hat{\Psi}_{ji}^k)^{B_l^K} = \mathcal{U}_{\Psi_j^k}$$

Previous Iterations, K_P:

$$\text{If} \quad (\bar{s}_{ji}^k)^{K_P} \cdot \left[(\bar{n}_i^k)^K - (\bar{n}_i^k)^{K_P} \right] = +1 \quad \text{then} \quad (\hat{\Psi}_{ji}^k)^{B_l^{K_P}} = \mathcal{L}_{\Psi_j^k}$$
$$\text{If} \quad (\bar{s}_{ji}^k)^{K_P} \cdot \left[(\bar{n}_i^k)^K - (\bar{n}_i^k)^{K_P} \right] = -1 \quad \text{then} \quad (\hat{\Psi}_{ji}^k)^{B_l^{K_P}} = \mathcal{U}_{\Psi_j^k}$$

Illustration – *conclusion*: The new set of x variables is defined as:

$$\hat{\Psi}_{11} = \hat{\Psi}_{12} = \Psi_1 \quad \text{and} \quad \hat{\Psi}_{21} = \hat{\Psi}_{22} = \Psi_2$$

Collecting the variables in n_i together gives the final Lagrange function as:

$$\begin{aligned} L^4(\boldsymbol{\Psi}, \boldsymbol{n}, \bar{\boldsymbol{\lambda}}) &= C - n_1\bar{\lambda}_1 - n_2\bar{\lambda}_2 \\ &+ \quad \{ n_1 - \bar{n}_1 \} \left\{ \hat{\Psi}_{11} \cdot \bar{\lambda}_1 + \hat{\Psi}_{21} \cdot \mathcal{G}_{12} \left[\tau_{12} + \bar{\lambda}_2 \right] \right\} \\ &+ \quad \{ n_2 - \bar{n}_2 \} \left\{ \hat{\Psi}_{12} \cdot \mathcal{G}_{21} \left[\tau_{21} + \bar{\lambda}_1 \right] + \hat{\Psi}_{22} \cdot \bar{\lambda}_2 \right\} \end{aligned}$$

Each term in n_i multiplies multiple a summation of terms involving the x variables. The bounds on these x variables are set in the manner just described in this section. □

4.5 Global Optimization Algorithm for the NRTL model

In what follows, k_S represents any node of the solution tree and the set of nodes is labeled N_{k_S}. k_t is a temporary node used in the generation of the set of previous Lagrange functions, $PL(K_P)$. $\mathcal{S}_C$ represents the current node under consideration at any given iteration and is obviously a leaf node. The subscript C denotes any parameter associated with the current iteration. The parent of a node is simply indicated by p. The set I_{k_S} represents the iteration number at which the particular node k_S is generated. The complete algorithm for the NRTL equilibrium model is now given.

STEP 0: Initialization

Select $\bar{\boldsymbol{n}}^0$ and ε. Set $K = 0$, $\mathcal{S}_C = R$, $k_S = \emptyset$, $P^U = +\infty$, $M^L = -\infty$.
Initialize $R_C\{\mathcal{L}^R, \mathcal{U}^R\}$ (viz. $\mathcal{L}^R_{n_i^k} = 0$; $\mathcal{U}^R_{n_i^k} = n^T$).

STEP 1: Primal Problem

Evaluate (P) to give $\hat{G}(\bar{\boldsymbol{n}}^K)$. Store $\bar{\boldsymbol{n}}^K, \bar{\boldsymbol{\lambda}}^K, (\bar{s}_{ji}^k)^K$.

If $\hat{G}(\bar{\boldsymbol{n}}^K) < P^U$ solve (NCF) locally to give $\hat{G}^*$.

Update $P^U = \min \left[P^U \ , \ \hat{G}(\bar{\boldsymbol{n}}^K) \ , \ \hat{G}^* \right]$

STEP 2: Select previous Lagrangians

Set $PL(K_P) = \emptyset$, $k_t = S_C$.

while $(\ k_t \neq R \ )$

do

$K_P = I_{k_t}$

$PL(K_P) = PL(K_P) \cup K_P$

$k_t = p\,(k_t)$

end

STEP 3: The Relaxed Dual Phase

(1) Choose a combination of qualifying constraints, B_l from the set CB.

Use $s_{ik}^{B_l}$ and $R_C\{\mathcal{L}^R, \mathcal{U}^R\}$ to calculate $B\{\mathcal{L}^B, \mathcal{U}^B\}$ and $\{\mathcal{L}_{\Psi_i^k}, \mathcal{U}_{\Psi_i^k}\}$.

Set $\hat{\boldsymbol{\Psi}}^{B_l^K}$ and $\hat{\boldsymbol{\Psi}}^{B_l^{K_P}}$ and solve the following problem (RD) to give μ_B^* and $\boldsymbol{n}^*$:

$$\left.\begin{array}{ll} \min & \mu_B \\ s.t. & \mu_B \geq L_C(\,\hat{\boldsymbol{\Psi}}^{B_l^K}, \boldsymbol{n}, \bar{\boldsymbol{\lambda}}^K) \\ & \mu_B \geq L(\,\hat{\boldsymbol{\Psi}}^{B_l^{K_P}}, \boldsymbol{n}, \bar{\boldsymbol{\lambda}}^{K_P}) \ \ \forall \ K_P \in PL(K_P) \\ & \mathcal{L}^B_{\boldsymbol{n}_i^k} \leq \ \ n_i^k \ \ \leq \ \mathcal{U}^B_{\boldsymbol{n}_i^k} \qquad \forall \ \ i \in C \ , \ k \in P_L \\ & \mathbf{0} = \mathbf{A} \cdot \mathbf{n} \ - \ \mathbf{b} \end{array}\right\} \qquad \text{(RD)}$$

where $L_C(\,\hat{\boldsymbol{\Psi}}^{B_l^K}, \boldsymbol{n}, \bar{\boldsymbol{\lambda}}^K)$ is given by Eqn. (39).

(i) If $\mu_B^* \geq P^U$, then fathom solution.

(ii) If $\mu_B^* < P^U$, then set $k_S = k_S + 1$, $p\,(k_S) = \mathcal{S}_C$, $I_{k_S} = K$, $\mu^{k_S} = \mu_B^*$, $\bar{n}^{k_S} = n^*$ and $R_{k_S}\{\mathcal{L}^R, \mathcal{U}^R\} = B\{\mathcal{L}^B, \mathcal{U}^B\}$.

(2) Choose another set of bounds B_l from CB and return to (1).

If there are no remaining unchosen B_l in CB, then proceed to Step 4.

STEP 4: Select mol vector for next iteration

$M^L = \underset{N_{k_S}}{\text{argmin}}\ \mu^{k_S}$; set $\mathcal{S}_C = k_S$, the associated node. Set $N_{k_S} = N_{k_S} \setminus \mathcal{S}_C$.

Set $\bar{n}^{K+1} = \bar{n}^{\mathcal{S}_C}$, $R_{K+1}\{\mathcal{L}^R, \mathcal{U}^R\} = R_{\mathcal{S}_C}\{\mathcal{L}^R, \mathcal{U}^R\}$.

STEP 5: Check for convergence

Check if $\left|\frac{P^U - M^L}{P^U}\right| \leq \epsilon$. If true, then STOP; otherwise set $K = K + 1$, and return to Step 1.

It has been shown how all the conditions required to guarantee ϵ-global convergence of the GOP algorithm are satisfied, and the proof is supplied in Floudas and Visweswaran [13, 14].

The main computational effort lies in solving the relaxed dual subproblems. There is a very simple way to reduce the number of connected variables. The material balance constraints appear affinely in the relaxed dual formulation. The material balance matrix represented by A has rank r so that r mol number variables can be written in terms of the others. In other words r connected variables are eliminated. Thus, the number of connected variables is now given as:

$$N_{CV} = \quad |C| \cdot |P| - \ r \tag{40}$$

For the phase equilibrium problem $r = |C|$. For cases where only liquid phases are considered, the material balance constraints are used to eliminate these r variables from interacting with the x variable set. This is shown in the illustrative example in the next section.

Another computational aid is the fact that at a given stage of the algorithm, if the current point matches a previous point for some (or all) $i \in C$, $k \in P_L$, then there is no need for a partitioning hyperplane in that dimension. This reduces the number of relaxed dual subproblems to be solved at that iteration. A significant number of relaxed dual subproblems are typically eliminated in this way.

4.6 Illustrative Example: n-Butyl-acetate – Water

The application of the GOP to a simple two component, two phase example is now considered. This illustrative example was studied by Heidemann and Mandhane [26] to demonstrate the potential complexities of the NRTL equation. It features two components, n-butyl-acetate (1) and water (2), at a temperature of 298K and a pressure of 1 atm. There are two possible liquid phases and they are modeled using the NRTL equation. Both phases share the same standard state, so that $\hat{G}_I$ as defined by Eqn. (9) supplies the Gibbs function to be minimized. The required binary parameters were obtained from Heidemann and Mandhane [26]:

$$\tau_{12} = 3.00498 \ , \ \tau_{21} = 4.69071 \quad \text{and} \quad \mathcal{G}_{12} = 0.30794 \ , \ \mathcal{G}_{21} = 0.15904$$

The nonrandomness constant used to calculate $\mathcal{G}_{ij}$ is $\alpha_{12} = \alpha_{21} = 0.39196$ The initial mixture charge is equimolar $(n_i^T = 0.5 \ \forall \ i)$ and no reaction occurs in the system. It appears to be a simple example but there are multiple stationary points and local solutions. In fact, there is a local minimum *and* a local maximum, in addition to the global solution. There is also a line of trivial solutions that represents physical one phase behavior, but mathematically yields two phase solutions, that is, the mol fractions are the same in each distinct phase. These solutions are given in Table 1 where the superscript I represents the first liquid phase. The mol numbers for the second liquid phase, denoted by the superscript II, are obtained as $n_i^{II} = n_i^T - n_i^I \ \forall \ i$. The Gibbs free energy surface as a function of the mol numbers in liquid phase I is pictured in Figure 4, where the various local solutions are shown, with the trivial solutions lying along the line defined by $n_1^I - n_2^I = 0$. Lin [29] employed a successive continuation method to solve the problem and trace all possible solution branches. In this manner, all the local and global extrema were obtained. However, there is no guarantee that a local solver will obtain the global solution, and the trivial solution or other local optima may be found. To illustrate this point, when (NCF) was solved using MINOS5.4 from 100 randomly selected starting points, the global solution was found in only 13 cases. The strong local minimum solution was found in 5 cases, and the trivial solution was obtained in the remaining 82 cases. This example therefore serves as an excellent demonstration tool for the proposed global optimization approach: it is challenging and it can be represented in three dimensional space.

In what follows the superscript I is dropped for the first liquid phase. The mass balance constraints are then given as:

$$n_1 + n_1^{II} = n_1^T \quad \text{and} \quad n_2 + n_2^{II} = n_2^T$$

These can be used to reduce the number of connected variables to $N_{CV} = 2$ by substituting them into the terms involving n_i^{II} within the curly braces of the Lagrange function defined by Eqn. (39). Thus, a maximum of four relaxed dual problems must be solved at each iteration. The convex portion of the objective function for the first liquid phase is defined as:

$$\mathcal{C}^1 = n_1 \ln \frac{n_1}{n_1 + n_2} + n_2 \ln \frac{n_2}{n_1 + n_2}$$

with $\mathcal{C}^{II}$ similarly defined for the second phase, then the explicit Lagrange function for use in the relaxed dual is as follows:

$$\begin{aligned} L(\boldsymbol{\Psi}, \boldsymbol{n}, \bar{\boldsymbol{\lambda}}) &= \mathcal{C} + \mathcal{C}^{II} - n_1\bar{\lambda}_1 - n_2\bar{\lambda}_2 - n_1^{II}\bar{\lambda}_1^{II} - n_2^{II}\bar{\lambda}_2^{II} \\ &+ \{n_1 - \bar{n}_1\} \cdot \left\{ \hat{\Psi}_{11}\bar{\lambda}_1 + \hat{\Psi}_{21}\mathcal{G}_{12}\left[\tau_{12} + \bar{\lambda}_2\right] - \hat{\Psi}_{11}^{II}\bar{\lambda}_1^{II} - \hat{\Psi}_{21}^{II}\mathcal{G}_{12}\left[\tau_{12} + \bar{\lambda}_2^{II}\right] \right\} \\ &+ \{n_2 - \bar{n}_2\} \cdot \left\{ \hat{\Psi}_{12}\mathcal{G}_{21}\left[\tau_{21} + \bar{\lambda}_1\right] + \hat{\Psi}_{22}\bar{\lambda}_2 - \hat{\Psi}_{12}^{II}\mathcal{G}_{21}\left[\tau_{21} + \bar{\lambda}_1^{II}\right] - \hat{\Psi}_{22}^{II}\bar{\lambda}_2^{II} \right\} \end{aligned}$$

Notice that the terms on the first line are convex with the linear terms involving $\bar{\boldsymbol{\lambda}}$ arising from the inclusion of the right hand side of Eqn. (26) in the Lagrange function. The interaction between the x and the y variable sets on the next two lines is purely bilinear. The derivatives of the Lagrangian with respect to the x variables yield linear functionalities in the y variables allowing the y space to be partitioned in a very simple manner.

<u>INITIALIZATION</u>: Choose a center starting point: $\bar{n}_1 = n_1^T/2 = 0.25$, $\bar{n}_2 = n_2^T/2 = 0.25$.

<u>ITERATION 1</u>: The initial parent n-rectangle, labeled $R\{\mathcal{L}^R, \mathcal{U}^R\}$, is defined as the complete feasible region and the primal is solved (a function evaluation) to give a first upper bound of -0.01758. All the relevant information is supplied in Table 2. The parent n-rectangle is divided into 4 box regions, and a relaxed dual problem is solved in each. These 4 regions are shown in Figure 5 where the larger solid dots signify the current point of the iteration, while the smaller solid dots represent the locations of the solutions of the relaxed dual problems in the relevant subdomains. For Iteration 1, the qualifying constraints are also explicitly supplied in Figure 5.

Region 1: The box bounds are: $0.25 \le n_1 \le 0.5$, $0.25 \le n_2 \le 0.5$. The x variable bounds in this box region as calculated from Eqns. (38) are given in Table 3. Their actual levels in the Lagrangian are given in Table 4. As an illustration of how these bounds are set, consider the x variable $\hat{\Psi}_{21}$: the quantity $(n_1 - \bar{n}_1)$ is positive in Region 1. In addition:

$$\mathcal{G}_{12}\left[\tau_{12} + \bar{\lambda}_2\right] = 0.7075 \; > \; 0$$

Therefore, the combined sign of this term will be positive. The x variable is set to its lower bound in this case, so that $\hat{\Psi}_{21} = \mathcal{L}^B_{\Psi_2} = 0.6189$, ensuring that the lower bound times a positive quantity will always provide a valid lower bound in the box region for this term. By performing the same analysis for each of the x variables, it is ensured that the Gibbs surface is validly underestimated in each box region of interest.

The Gibbs surface in this region is shown in Figure 6 along with its underestimating Lagrangian. Notice that (i) the Lagrangian matches the Gibbs surface at the current point $\bar{n} = \{0.25, 0.25\}$, (ii) that it underestimates the Gibbs surface at all points, and (iii) that it is clearly convex. The solution of the relaxed dual lies in the bottom left hand corner of Figure 6 at a vertex of the box region, and is given as:

$$n_1^* = n_2^* = 0.5 \quad \text{with} \quad \mu_1^* = -0.4261$$

Region 2: The box bounds are: $0 \le n_1 \le 0.25$, $0.25 \le n_2 \le 0.5$. The Gibbs energy surface and the corresponding Lagrangian are shown in Figure 7. In this case the solution lies in the interior of the box region and is:

$$n_1^* = 0.1028 \; , \; n_2^* = 0.3972 \quad \text{with} \quad \mu_2^* = -0.2303$$

Region 3: The box bounds are: $0.25 \leq n_1 \leq 0.5$, $0 \leq n_2 \leq 0.25$. The solution is given as follows:

$$n_1^* = 0.3972 \ , \ n_2^* = 0.1028 \quad \text{with} \quad \mu^* = -0.2303$$

Region 4: The box bounds are: $0 \leq n_1 \leq 0.25$, $0 \leq n_2 \leq 0.25$ with solution:

$$n_1^* = 0 \ , \ n_2^* = 0 \quad \text{with} \quad \mu^* = -0.4261$$

Note that Regions 3 and 4 yield the same lower bounds as Regions 2 and 1 respectively and that the y variable levels in these regions are equal to $\{n_i^T - n_i^*\}$ where $\{n_i^*\}$ represents the appropriate solution from either Region 1 or 2. This is due to the fact that a starting point in the center of the feasible region was chosen so that the Lagrangian yields equivalent expressions for $\{n_i\}$ as for $\{n_i^T - n_i\}$, implying that Regions 3 and 4 may be discarded from future consideration. For other starting points this property will not hold.

<u>ITERATION 2</u>: The infimum of all obtained relaxed dual solutions supplies the parent region for this iteration as Region 1 of Iteration 1, with a lower bound of -0.4261. This solution is then deleted from the candidate set of lower bounds. All information in regard to the primal is given in Table 2. The current point is $\bar{n} = \{0.5, 0.5\}$ and thus the upper bound given by the primal does not change, that is, it also lies along the hyperplane of trivial solutions. Only one region need be considered in this case as the current point lies on a vertex of the parent region. For this reason, the box region is the same as it was for Region 1 of Iteration 1 as shown in Figure 5. Two Lagrange functions are required and superscripts on brackets indicate iteration number. For the Lagrange function to be generated from the first iteration, $(\bar{n}_i)^2 - (\bar{n}_i)^1 = 0.5 - 0.25 > 0$ for $i = 1, 2$. $n_i - (\bar{n}_i)^2 = n_i - 0.5 < 0$ for the current iteration. By way of illustration, for the Lagrange function of the first iteration, $(\hat{\Psi}_{11})^1 = \mathcal{U}_{\Psi_1} = 0.9263$ as $(\bar{\lambda}_1)^1 < 0$ and $n_i - 0.25 > 0$; while for the current iteration, $(\hat{\Psi}_{11})^2 = \mathcal{L}_{\Psi_2} = 0.7587$ as $(\bar{\lambda}_1)^2 < 0$ and $n_i - 0.5 < 0$. For both these cases, $(\bar{\lambda}_1)^K < 0$. The Gibbs surface and the supremum of the Lagrangian generated in Region 1 of Iteration 1 and the current one are plotted in Figure 8. The solution lies in the interior of the feasible region:

$$n_1^* = 0.3796 \ , \ n_2^* = 0.3704 \quad \text{with} \quad \mu_3^* = -0.2221$$

This lower bound lies below the current best upper bound and is added to the set of relaxed dual solutions.

<u>ITERATION 3</u>: Region 2 of Iteration 1 contains the infimum of all remaining lower bounds as -0.2303 and is deleted from the set of candidate solutions. The new parent region is therefore defined as: $0 \leq n_1 \leq 0.25$, $0.25 \leq n_2 \leq 0.5$, with a current point $\bar{n} = \{0.1028, 0.3972\}$. This point yields a primal value of 0.00507 implying that the current best upper bound does not change. It is divided into 4 box regions as is illustrated in Figure 5. The box bounds for these regions along with the corresponding solutions are supplied in Table 5. The locations of these solutions in the y

variable space can also be seen in Figure 5. There are two Lagrangians for each box region, one from Region 2 of Iteration 1 which is the same for all 4 box regions, and one from the current iteration. The supremum of both these Lagrangians is plotted for all 4 regions along with the Gibbs surfaces in Figure 9.

ITERATION 4: The infimum of all remaining lower bounds is obtained from Iteration 2 as -0.2221. This solution is then deleted from the set of relaxed dual lower bounds. The parent region for this iteration is defined as: $0.25 \leq n_1 \leq 0.5$, $0.25 \leq n_2 \leq 0.5$, with a current point $\bar{n} = \{0.3796, 0.3704\}$. This point yields a primal value of -0.01754 so the current best upper bound does not change. 4 relaxed dual problems must be solved and each of these contains 3 Lagrangians, two constructed from Iterations 1 and 2 (common to all 4 subproblems), and a third which is based on the particular box region under consideration. The box bounds are given in Table 6 together with the solutions of each of the relaxed dual problems. The 4 box regions and the location of these solutions is shown in Figure 5.

For Iteration 5, the next parent region is given by Region 1 of Iteration 4, which is the infimum of all available relaxed dual solutions. 4 relaxed dual problems are again solved, each containing 3 Lagrange functions. The algorithm proceeds in this manner until the infimum of all the remaining lower bounds is within $\epsilon = 0.0005$ of the best upper bound. For this particular problem and starting point, convergence occurs after 107 iterations. A local solver will *not* converge to the global solution from the initial point considered above. The progress of the upper and lower bounds is charted in Table 7. The total cpu time required was 1.23 sec, and a total of 359 relaxed dual subproblems were solved. 57% of these solutions were fathomed.

4.7 Examples

Before discussing the examples, some general comments in relation to the problems and systems considered are now made:

(i) All computational runs were performed on a Hewlett Packard 9000/730 machine. The GOP is implemented in C as part of the package GLOPEQ (GLobal Optimization for the Phase and chemical EQuilibrium problem). MINOS5.4 is accessed as a subroutine. The cpu times reported represent the total real time taken by the algorithm. Unless otherwise stated, convergence is deemed to have occurred when the relative tolerance is less than $\epsilon = 0.0005$. This tight a tolerance ensures that that global solution is generated well before final convergence occurs.

    It should be noted that GLOPEQ can be used to minimize the Gibbs free energy function when the liquid phase nonidealities are modeled using the Wilson, T–K–Wilson, UNIQUAC, UNIFAC and ASOG equations. GLOPEQ is also capable of obtaining the minimum of the tangent plane distance function for any of these equations. The tangent plane stability analysis originally introduced by Gibbs [20, 21] is a very useful way of determining if a postulated solution is the equilibrium one. For this set of problems, $N_{CV} = |C| - 1$, so that the number of connected variables is of the order of components in the system rather than the number of components times phases. This makes it possible to verify equilibrium solutions for systems with a larger number of components in significantly reduced computational time. The same properties developed here are also applicable for minimizing the tangent plane distance function for nonideal liquid phases modeled by the NRTL equation. McDonald and Floudas [35] describe the global optimization approach for the tangent plane criterion for systems modeled using the NRTL or UNIQUAC equation. In addition, GLOPEQ utilizes the minimization of the Gibbs free energy in *conjunction* with the tangent plane stability analysis to generate equilibrium solutions for all the above activity coefficient correlations as efficiently as possible, as well as being able to solve these optimization problems individually. This is fully described in McDonald and Floudas [34].

(ii) Any problem where more than one liquid phase is postulated will have a degenerate set of trivial solutions where the component mol fractions in each of the liquid phases are the same. If one of these points is used to initiate the search for a solver such as MINOS5.4, then it will be unable to move from the trivial solution because it corresponds to a local minimum. This characteristic has already been observed in the illustrative example. All the examples in this section show such behavior and this has proven to be a major problem for Newton–based local optimization algorithms. The results show that in all cases, the GOP successfully obtains the global solution when supplied with such a trivial solution initial point.

(iii) If no reaction occurs in the system, then $\hat{G}_I$ or $\hat{G}_{II}$, as defined by Eqn. (9) and Eqn. (11) respectively, are the forms of the objective function that will be minimized. Unless otherwise stated, the saturated pressures for all compounds are calculated from the tabulations of Reid *et al.* [47].

(iv) For a nonreacting system where the temperature and pressure are specified, the maximum possible number of phases present at equilibrium is equal to the number of components in the system. For the examples considered in this work, this means that there are a maximum of two liquid phases and a potential vapor phase because the conditions under consideration are in the vicinity of the bubble point.

(v) It is possible to incorporate a simple local search technique into the framework of the global optimization algorithm. If the primal function value is less than the current best upper bound at any given iteration, MINOS5.4 is used to solve (NCF) as a nonconvex nonlinear programming problem, using the current mol numbers $\{\bar{n}_i^k\}$ as a starting point. If the resulting solution supplies a Gibbs free energy level less than the current best upper bound, then P^U is updated to equal this new solution. This is done because typically a point close to the global solution is generated at a relatively early stage of the algorithm, but this solution is not refined until a later point in the solution procedure. The advantages of such a strategy are obvious: immediate refinement of solutions (local or global) will occur with the attractive benefit of improved upper bounds at an earlier stage of the algorithm. This also means a greater number of solutions will be fathomed. In summary, the local search is an efficient way in which to generate valid and improved upper bounds, independently of the global optimization algorithm. Regardless of whether this technique is used, the global solution will be generated in the same number of iterations.

(vi) When a solution is obtained that contains liquid phase(s) only, a stability check on an incipient ideal vapor phase is performed to establish if the obtained solution is stable with respect to the formation of a vapor phase. This is described in more detail below.

Stability criterion for the vapor phase: If the *global* solution in a nonreacting system involving liquid phase(s) has been obtained, where the mol fractions in one of the liquid phases are labeled $\boldsymbol{z} \equiv \{z_i\}$, then a necessary and sufficient condition (Baker *et al.* [1]) for the stability of this solution with respect to the potential formation of a vapor phase is that the following function, $F(\boldsymbol{y})$, be nonnegative for all feasible values of mol fractions:

$$F(\boldsymbol{y}) \;=\; \sum_{i \in C} y_i \left\{ \mu_i(\boldsymbol{y}) - \mu_i^0(\boldsymbol{z}) \right\} \geq 0 \tag{41}$$

where $\boldsymbol{y} \equiv \{y_i\}$ are the vapor mol fraction variables of the formulation, $\mu_i(\boldsymbol{y})$ is the chemical potential of the vapor phase at composition $\boldsymbol{y}$, and $\mu_i^0(\boldsymbol{z})$ is the chemical potential of the liquid phase for component i at mol fraction $\boldsymbol{z}$ with $\gamma_i(\boldsymbol{z})$ calculated from Eqn. (17).

Lemma 4.1 *Define the function $\mathcal{F}(\boldsymbol{y})/RT$ with $\boldsymbol{y} > 0$ as follows:*

$$\frac{\mathcal{F}(\boldsymbol{y})}{RT} = \sum_{i \in C} y_i \left\{ \ln P y_i - \ln P_i^{SAT} \cdot \gamma_i(z) \cdot z_i \right\} \tag{42}$$

then $\mathcal{F}(\boldsymbol{y})/RT$ is convex.

Proof: The quantity $y_i \ln y_i$ is convex. A summation of these terms will also be convex. The pressure term can be extracted from the logarithmic term and therefore appears linearly in the formulation along with the chemical potential terms for the liquid phase, $\mu_i^0(z)$. The summation of convex and linear terms will itself be convex, i.e. $\mathcal{F}(\boldsymbol{y})/RT$ is convex. □

Note that in progressing from Eqn. (41) to Eqn. (42), Eqn. (10) has been used so that the terms involving $\Delta G_i^{V,f}$ cancel. If (S) is designated as the following formulation:

$$\min \; \frac{\mathcal{F}(\boldsymbol{y})}{RT} \quad s.t. \quad \sum_{i \in C} y_i = 1 \;\;,\;\; 0 \leq y_i \leq 1 \quad \forall \, i \in C \tag{S}$$

then it is clear that any local solution of (S) will be a global one due to Lemma 4.1 because the objective function and the feasible region are convex. This implies that a local solver can be used to obtain global solutions to (S). Note that for any given phase configuration involving liquid phases, the resulting solution as obtained by using the GOP is guaranteed to be global. Theorem 3 of Baker *et al.* [1] proves that if the solution of (S) yields a nonnegative objective function level, then a vapor phase will positively not form. In the case where it is unknown if the liquid phase solution is a global one. this claim cannot be made and represents an important advantage of the proposed approach as it is possible to perform a globally valid stability check for the vapor phase. If the optimal value is negative, then a vapor phase must be postulated and the equilibrium calculations reworked. Unlike other methods that utilize the results from solving the stability problem, the global approach described here does *not* use the results obtained from solving (S). Rather, a global optimization problem involving the vapor phase is solved to obtain the equilibrium solution.

4.7.1 Example 1: LL Equilibrium for Toluene – Water

The first example is a binary one involving toluene and water taken from Castillo and Grossmann [10]. The conditions are 298K and 1 atm pressure. There are two postulated liquid phases sharing the same standard state so that $\hat{G}_I$ given by Eqn. (9) is the objective function to be minimized. The nonconvexities of the problem are relatively weak, but it does posses a degenerate line of trivial solutions where a mathematical two phase solution is found, corresponding to a single phase physical solution. A local solver such as MINOS5.4 will fail to move from this local solution if it is used to initiate the search. The binary parameters are obtained from Bender and Block [2] as:

$$\tau_{12} = 4.93 \ , \ \tau_{21} = 7.77 \ , \ \alpha_{12} = \alpha_{21} = 0.2485$$

An equimolar charge is assumed (0.5 mol for each component) and no reaction takes place in the system. There are a total of 4 connected variables for this problem. However, it is possible to eliminate the variables of the second phase through the mass balance constraints, i.e. $n_i^{II} = n_i^T - n_i^I$ for $\{i_1, i_2\}$. The number of connected variables is then given as:

$$\begin{aligned} N_{CV} &= |C| \cdot |P| \quad - \quad r \\ &= 2 \cdot 2 - 2 \ = \ 2 \end{aligned}$$

Thus, a maximum of $2^2 = 4$ relaxed dual subproblems must be solved at each iteration.

From a starting point in the center of the feasible region, the GOP algorithm converges to the global solution in 7 iterations, and the solution is given in Table 8. From this initial point, a local solver may be unable to find the global solution. For example, any Newton–based method will not move from this local minimum. Only 23 relaxed dual subproblems were solved and 13 of these were fathomed (i.e. the supplied lower bounds lay above the current best upper bound). The total time taken to obtain the global solution was 0.07 cpu sec.

4.7.2 Example 2: LL Equilibrium for Toluene – Water – Aniline

This example consists of a non-reacting three component system and was investigated by Castillo and Grossmann [10]. The system is at a temperature of 298K and a pressure of 1 atm. Both liquid phases are modeled using the NRTL activity coefficient equation. The parameters for this model were obtained from Bender and Block [2] and are supplied in Table 9. There are two potential liquid phases so that the adjusted objective function, $\hat{G}_I$, defined by Eqn. (9) will be used. The feed charge is given in Table 10. No reaction occurs so that the rank of the material balance matrix is given by the number of components. The number of connected variables is then:

$$\begin{aligned} N_{CV} &= |C| \cdot |P| - \quad r \\ &= 3 \cdot 2 - 3 \\ &= 3 \end{aligned}$$

This implies that there are $2^3 = 8$ relaxed dual subproblems to be solved at every iteration.

This example displays strong trivial solution convergence characteristics as pointed out by Paules and Floudas [44]. In applying the GOS technique, Paules and Floudas [44] found that convergence to the correct solution could still not be guaranteed for all starting points. A variety of restart techniques were invoked and extra Lagrangians were included to avoid convergence to the metastable trivial solution. Using these aids, only one starting point failed to converge to the non-trivial solution. In this work, when (NCF) was solved locally as a nonconvex programme using MINOS5.4, convergence to the trivial solution occurred for 13 out of 100 randomly generated initial points. These difficulties are in large part due to having two phases described by exactly the same mathematical equations, so that a local technique will have difficulty moving from the hyperplane of trivial solutions.

Supplied with an initial trivial solution, the algorithm converges to the global solution in 74 iterations. A total of 461 relaxed dual subproblems were solved and the percentage of total fathomed solutions was 82%. The optimal solution is given in Table 10, featuring a toluene-rich phase and a water-rich phase. When the stability problem (S) was solved using this global solution, it was found to be stable with respect to the incipient vapor phase.

4.7.3 Example 3: LL Equilibrium for n-Propanol – n-Butanol – Water

This system was one of two studied by Block and Hegner [3] in their modeling of three phase distillation towers. n-Butanol and water form the only partially miscible binary pair (i.e. it is a Type I system) with a relatively small domain of immiscibility. The binary parameters as obtained by them for use in the NRTL equation are supplied in Table 11. $\hat{G}_{II}$ supplies the objective function to be minimized, and $N_{CV} = 3$. Block and Hegner [3] conducted the liquid phase splitting computations independently of the vapor phase i.e. the parameters have no dependence on temperature. It is therefore meaningless to consider a vapor phase for this example. Walraven and van Rompay [63] subsequently used this problem in order to test their phase splitting algorithm for a number of different feed charges.

Two source feeds from the work of Walraven and van Rompay [63] were examined, and these charges are given in Table 12. The first of these lies well within the immiscibility region – $\{n_i^T\} = \{0.04, 0.16, 0.80\}$ – and therefore causes little problem for a local solver. However, the second considered source charge of $\{n_i^T\} = \{0.148, 0.052, 0.800\}$ lies close to the plait point, an area in which it is notoriously difficult to obtain the correct equilibrium solution. The trivial solution objective function value is -1.1919705, while the two phase global solution has an objective function value of -1.1919716, a difference of only $1.1 \cdot 10^{-6}$! Solving (NCF) using MINOS5.4 succeeded in obtaining the global solution from only 8 out of 100 random starting points. Nonetheless, the GOP algorithm generated the global solution for this very difficult problem when supplied with a trivial solution starting point. This clearly demonstrates the effectiveness of the algorithm in generating global solutions for extremely challenging problems.

The equilibrium solutions for the two sets of conditions considered here are given in Table 12, along with some selected computational results. N_I is the number of iterations required to converge to the global solution, and N_F is the percentage of solutions that are fathomed. The difficulty of the problem when the source charge is close to the plait point is evident in the increased computational effort required to obtain the equilibrium solution for this case.

4.7.4 Example 4: LL Equilibrium for Ethanol – Ethyl acetate – Water

This system was the second example studied by Walraven and van Rompay [63]. Soares *et al.* [53] also examined this system in their analysis of three phase flash calculations and supplied the constants for use in the Antoine equation. The NRTL binary parameters were supplied by van Zandijcke and Verhoeye [59] and are given in Table 13. Ethyl-acetate–water is the single partially miscible binary pair of the system (i.e. a Type I system). The objective function is given by $\hat{G}_{II}$ with $N_{CV} = 3$. A single source feed was selected from Walraven and van Rompay [63], with $\{n_i^T\} = \{0.04, 0.30, 0.66\}$ at a temperature of 343.15K. The algorithm shows similar performance for the other sets of feed charges and are therefore not reported here.

The global solution is given in Table 14 along with its associated computational requirements. A stability analysis on a perturbing ideal vapor phase reveals that the LL configuration is stable with respect to the potential formation of a vapor phase.

4.7.5 Example 5: LL Equilibrium for n-Butanol – Water – n-Butyl-acetate

This example was studied by Block and Hegner [3] to simulate a column that utilizes a top phase separator. A water rich stream is removed at the top of the column and the organic phase is refluxed back to the column. The NRTL binary parameters are given in Table 15. These parameters are temperature independent as was the case in Example 3 so there is no need to consider a vapor phase. The problem was solved for the conditions in the top phase separator and the corresponding feed charge is $\{n_i^T\} = \{0.14, 0.64, 0.22\}$, as shown in Table 16. $\hat{G}_{II}$ defined the objective function that was minimized and $N_{CV} = 3$.

The global solution for the feed charge under consideration is supplied in Table 16. The water rich phase composes 52% of the top phase separator exit stream. The algorithm took 105 iterations and a total time of 2.01 cpu sec to obtain this solution. The fathoming rate was 67%.

4.7.6 Example 6: LLV Equilibrium for Benzene – Acetonitrile – Water

This example is taken from Castillo and Grossmann [10]. It features three components involving a liquid phase, a vapor phase, and a potential second liquid phase. The parameters for the NRTL are supplied in the original work of Castillo and Grossmann [10]. They supply values for $g_{ij} - g_{jj}$ so that τ_{ij} is calculated using Eqn. (18) with $R = 1.9872$ cal/K/mol. Table 17 supplies the parameters for use in the equation $\mathcal{G}_{ij} = \exp(-\alpha_{ij}\tau_{ij})$. Three sets of conditions are considered in this work.

Conditions (A): $T = 333$K , $P = 0.769$ atm

In this work, an LLV global solution is obtained and is given in Table 19 along with a local LL solution. The mol fractions of the equilibrium solution obtained here agree reasonably well with those reported by Castillo and Grossmann [10], although the amount of mols in each phase differs significantly. There are six connected variables for this example, meaning that a maximum of 64 relaxed dual subproblems must be solved at each iteration, but typically a much fewer number of subproblems are solved. Using a relative convergence tolerance of 0.001, the global solution was obtained in 5842 iterations, consuming a total time of 766 cpu sec. 94% of the solutions were fathomed.

Conditions (B): $T = 333$ K , $P = 1$ atm

In this case, the pressure is too high to favor the formation of a vapor phase and an LL solution is obtained, as shown in Table 19. It should be noted that this solution also corresponds to a local LL solution for *Conditions (A)*. This solution was obtained in 52 iterations consuming a total time of 1.19 cpu sec. The fathoming rate was 77%. The solution obtained here agreed very closely with that provided by Castillo and Grossmann [10], suggesting that the discrepancies of the results reported here for *Conditions (A)* and *Conditions (C)* are due to the vapor phase. A stability check for an incipient vapor phase gave a solution of zero, confirming that a vapor phase is *not* present at the equilibrium solution.

Conditions (C): $T = 300$K , $P = 0.1$ atm

This work finds an LV equilibrium solution which is given in Table 20 along with another local LL solution. An LV solution is also reported by Castillo and Grossmann [10] and Lantagne *et al.* [28] and the results are in good agreement. If two liquid phases and a single vapor phase are postulated, then the GOP algorithm takes 655 iterations and a total time of 118 cpu sec to converge to the global solution with a fathoming rate of 86%. If a single liquid phase is postulated so that $N_{CV} = 3$, then convergence occurs in 34 iterations taking 0.88 cpu sec ($\epsilon = 0.0001$).

4.7.7 Example 7: LV Esterification Reaction

This example involves the esterification reaction between ethanol and acetic acid to form ethyl acetate and water. It has been used extensively in the literature to test a variety of equilibrium calculation methods including those of Sanderson and Chien [50], George *et al.* [19], Castillo and Grossmann [10], Lantagne *et al.* [28], Castier *et al.* [9], Xiao *et al.* [66], Gautam and Seider [17] and Paules and Floudas [44]. Suzuki *et al.* [57] obtained the binary parameters for use in the Wilson activity coefficient equation, and these parameters account for the formation of dimers and trimers of acetic acid in the vapor phase. All the above authors use this set of parameters except for Xiao *et al.* [66]. In this case, the UNIQUAC equation was employed with parameters derived from the UNIFAC model of Fredenslund *et al.* [15]. However, this does not account for the polymerization of acetic acid in the vapor phase.

In this work, binary parameters are required for the NRTL equation and these are obtained from infinite dilution activity coefficient information. An estimate of these quantities for each binary pair can be obtained from the Wilson equation as:

$$\ln \gamma_1^\infty = 1 - \ln \Lambda_{12} - \Lambda_{21} \quad \text{and} \quad \ln \gamma_2^\infty = 1 - \ln \Lambda_{21} - \Lambda_{12}$$

where Λ_{ij} is the Wilson interaction parameter for the binary $i - j$ obtained from Suzuki *et al.* [57]. $\alpha_{ij} = 0.3$ provides a reasonable estimate for the nonrandomness constant for all binary pairs and on this basis, unique values can be determined for τ_{12} and τ_{21} (see Renon and Prausnitz [49]) using the following pair of equations:

$$\tau_{12} = \ln \gamma_2^\infty - \tau_{21} \exp\left(-\alpha_{12}\tau_{21}\right) \quad \text{with} \quad \tau_{21} = \ln \gamma_1^\infty - \tau_{12} \exp\left(-\alpha_{12}\tau_{12}\right)$$

The values of τ_{ij} obtained by this procedure are provided in Table 21. The elemental abundance matrix, a_{ei}, as well as the vector of total amounts of the elements, b_e, are supplied in Table 22.

The Gibbs free energies of formation for the vapor phase were calculated by integrating the van't Hoff equation. Kirchoff's equation was used to calculate the enthalpies of formation with the required heat capacity data taken from Reid *et al.* [46]. Table 23 supplies the Gibbs free energies of formation for the vapor phase. The Gibbs free energy of formation for the liquid phase was calculated using Eqn. (10) with the parameters for use in the Antoine equation taken from Xiao *et al.* [66].

There are 4 connected variables for this example so that a maximum of 16 relaxed dual subproblems are solved at each iteration. At a temperature of 355K and for a relative convergence tolerance of 0.00005, the LV global solution is obtained in 173 iterations taking a total time of 8.53 cpu sec. The fathoming rate was 60%. The equilibrium solution is given in Table 23. Because the vapor phase is assumed to behave ideally, the chemical reaction equilibrium constant, K_r is expressed as:

$$K_r = \frac{y_{EtAc}\, y_{H_2O}}{y_{EtOH}\, y_{HAc}} = 33.13$$

This agrees well with the value of 33.55 reported by Xiao *et al.* [66] despite the fact that the interaction coefficients were obtained in a rudimentary manner. The compositions also agree reasonably well.

At a temperature of 358K, the liquid phase disappears. The Gibbs free energies of formation for the vapor phase at this temperature are given in Table 24, along with the mol fractions at equilibrium for the vapor phase global solution. In this case $K_r = 31.80$ which agrees closely with the value of 31.75 computed by George *et al.* [19]. With a liquid and a vapor phase postulated, the GOP algorithm computes the equilibrium vapor phase solution in 54 iterations, with a total cpu time of 3.7 sec.

5 Conclusions

A global optimization algorithm has been proposed to solve the phase and chemical equilibrium problem when the liquid phase can be modeled by the NRTL equation and the vapor phase is considered ideal. The proposed approach guarantees finding the global solution for this class of problems. A simplification of the objective function was provided that should prove very useful when employing the NRTL equation. Transformation variables were introduced in order to induce the structure required by the GOP algorithm to assure convergence to an ϵ-global solution. This structure features a biconvex objective function subject to a bilinear set of equality constraints. Numerous examples were presented which demonstrate the effectiveness of the algorithm in solving several phase equilibrium problems of varying degrees of difficulty. For systems that can be modeled using the Wilson, T-K-Wilson, UNIQUAC, UNIFAC and ASOG equations, new properties have been derived which allow the application of a branch and bound global optimization algorithm to also guarantee obtaining ϵ-global solutions. McDonald and Floudas [33] provide the analysis for the UNIQUAC equation. The package GLOPEQ uses the minimization of the Gibbs free energy in tandem with the tangent plane stability analysis to guarantee obtaining equilibrium solutions for all systems that can be modeled using the equations listed above, as described by McDonald and Floudas [34].

Acknowledgement: The authors gratefully acknowledge financial support from the National Science Foundation under Grants CBT-8857013 and CTS-9221411, as well as support from Amoco Chemical Co., Exxon Co., Tennessee Eastman Co., Mobil Co., and Shell Development Co.

References

[1] L.E. Baker, A.C. Pierce, and K.D. Luks, Gibbs energy analysis of phase equlibria, *Soc. Petro. Eng. J.*, page 731, October 1982.

[2] E. Bender and U. Block, Thermodynamische berechnung der flüssig-flüssig-extraktion, *Verfahrenstechnik*, 9(3):106, 1975.

[3] U. Block and B. Hegner, Development and application of a simulation model for three-phase distillation, *AIChE J.*, 22(3):582, 1976.

[4] S.R. Brinkley, Calculation of the equilibrium composition of systems of many constituents, *J. Chem. Phys.*, 15:107, 1947.

[5] B.P. Cairns and I.A. Furzer, Multicomponent three-phase azeotropic distillation. 1. Extensive experimental data and simulation results, *I&EC Res.*, 29:1349, 1990.

[6] B.P. Cairns and I.A. Furzer, Multicomponent three-phase azeotropic distillation. 2. Phase-stability and phase-splitting algorithms, *I&EC Res.*, 29:1364, 1990.

[7] B.P. Cairns and I.A. Furzer, Multicomponent three-phase azeotropic distillation. 3. Thermodynamic models and multiple solutions, *I&EC Res.*, 29:1383, 1990.

[8] H.S. Caram and L.E. Scriven, Non-unique reaction equilibria in non-ideal systems, *Chem. Eng. Sci.*, 31:163, 1976.

[9] M. Castier, P. Rasmussen, and A. Fredenslund, Calculation of simultaneous chemical and phase equilibria in nonideal systems, *Chem. Eng. Sci.*, 44(2):237, 1989.

[10] J. Castillo and I.E. Grossmann, Computation of phase and chemical equilibria, *Comput. chem. engng.*, 5:99, 1981.

[11] P.T. Eubank, A.E. Elhassen, M.A. Barrufet, and W.B. Whiting, Area method for prediction of fluid-phase equilibria, *I&EC Res.*, 31:942, 1992.

[12] C.A. Floudas, A. Aggarwal, and A.R. Ciric, A global optimum search for nonconvex NLP and MINLP problems, *Comput. chem. engng.*, 13(10):1117, 1989.

[13] C.A. Floudas and V. Visweswaran, A global optimization algorithm (GOP) for certain classes of nonconvex NLPs: I. Theory, *Comput. chem. engng.*, 14(12):1397, 1990.

[14] C.A. Floudas and V. Visweswaran, A primal-relaxed dual global optimization approach, *Journal of Optimization Theory and Applications*, 78(2):187, 1993.

[15] A. Fredenslund, J. Gmëhling, and P. Rasmussen, Vapor–liquid equilibria using UNIFAC, Elsevier, Englewood Cliffs, New Jersey, 1977.

[16] R. Gautam and W.D. Seider, Computation of phase and chemical equilibrium, Part I: Local and constrained minima in Gibbs free energy, *AIChE J.*, 25(6):991, 1979.

[17] R. Gautam and W.D. Seider, Computation of phase and chemical equilibrium, Part II: Phase-splitting, *AIChE J.*, 25(6):999, 1979.

[18] R. Gautam and W.D. Seider, Computation of phase and chemical equilibrium, Part III: Electrolytic solutions, *AIChE J.*, 25(6):1006, 1979.

[19] B. George, L.P. Brown, C.H. Farmer, P. Buthod, and F.S. Manning, Computation of multicomponent, multiphase equilibrium, *Ind. Eng. Chem. Proc. Des. Dev.*, 15(3):372, 1976.

[20] J.W. Gibbs, Graphical methods in the thermodynamics of fluids, *Trans. Connecticut Acad.*, 2:311, May 1873.

[21] J.W. Gibbs, A method of geometrical representation of the thermodynamic properties of substances by means of surfaces, *Trans. Connecticut Acad.*, 2:382, May 1873.

[22] S. Gordon and B.J. McBride, Computer program for calculation of complex chemical equilibrium compositions, rocket performance, incident and reflected shocks, and Chapman-Jouguet detonations, *NASA SP-273*, 1971.

[23] H. Greiner, An efficient implementation of Newton's method for complex nonideal chemical equilibria, *Comput. chem. engng.*, 15(2):115, 1991.

[24] I.E. Grossmann and J. Davidson, Computation of restricted chemical equilibria, *Comput. chem. engng.*, 6(2):181, 1982.

[25] R.A. Heidemann, Non-Uniqueness in phase and reaction equilibrium computations, *Chem. Eng. Sci.*, 33:1517, 1978.

[26] R.A. Heidemann and J.M. Mandhane, Some properties of the NRTL equation in correcting liquid-liquid equilibrium data, *Chem. Eng. Sci.*, 28:1213, 1973.

[27] J.W. Kovach and W.D. Seider, Heterogeneous azeotropic distillation: experimental and simulation results, *AIChE J.*, 33(8):1300, 1987.

[28] G. Lantagne, B. Marcos, and B. Cayrol, Computation of complex equilibria by nonlinear optimization, *Comput. chem. engng.*, 12(6):589, 1988.

[29] W.J. Lin, Application of continuation and modeling methods to phase equilibrium, steady-state and dynamic process calculations, PhD thesis, University of Utah, 1988.

[30] W.B. Liu and C.A. Floudas, A remark on the GOP algorithm for global optimization, *Journal of Global Optimization*, 3:519, 1993.

[31] A. Lucia and J. Xu, Chemical process optimization using Newton-like methods, *Comput. chem. engng.*, 14(2):119, 1990.

[32] D.W. Marquardt, An algorithm for least-square estimation of nonlinear parameters, *J. Soc. Ind. Appl. Math.*, 35:431, 1963.

[33] C.M. McDonald and C.A. Floudas, Decomposition based and branch and bound global optimization approaches for the phase equilibrium problem, *Journal of Global Optimization*, 1994, in press.

[34] C.M. McDonald and C.A. Floudas, GLOPEQ: A new computational tool for the phase and chemical equilibrium problem, 1994, in preparation.

[35] C.M. McDonald and C.A. Floudas, Global optimization for the phase stability problem, May, 1994, accepted by *AIChE J.*

[36] M.L. Michelsen, The isothermal flash problem - Part I. Stability, *Fluid Phase Equilibria*, 9:1, 1982.

[37] M.L. Michelsen, The isothermal flash problem - Part II. Phase-split calculation, *Fluid Phase Equilibria*, 9:21, 1982.

[38] N.R. Nagarajan, A.S. Cullick, and A. Griewank, New strategy for phase equilibrium and critical point calculations by thermodynamic energy analysis. Part I. Stability analysis and flash, *Fluid Phase Equilibria*, 62:191, 1991.

[39] N.R. Nagarajan, A.S. Cullick, and A. Griewank, New strategy for phase equilibrium and critical point calculations by thermodynamic energy analysis. Part II. Critical Point Calculations, *Fluid Phase Equilibria*, 62:211, 1991.

[40] M.O. Ohanomah and D.W. Thompson, Computation of multicomponent phase equilibria - Part I. Vapour-liquid equilibria, *Comput. chem. engng.*, 8(3/4):147, 1984.

[41] M.O. Ohanomah and D.W. Thompson, Computation of multicomponent phase equilibria - Part II. Liquid-liquid and solid-liquid equilibria, *Comput. chem. engng.*, 8(3/4):157, 1984.

[42] M.O. Ohanomah and D.W. Thompson, Computation of multicomponent phase equilibria - Part III. Multiphase equilibria, *Comput. chem. engng.*, 8(3/4):163, 1984.

[43] H.G. Othmer, Nonuniqueness of equilibria in closed reacting systems, *Chem. Eng. Sci.*, 31:993, 1976.

[44] G.E. Paules, IV and C.A. Floudas, A new optimization approach for phase and chemical equilibrium problems, Paper presented at the Annual AIChE Meeting, San Franciso, CA, November, 1989.

[45] M.J.D. Powell, A new algorithm for unconstrained optimization: Nonlinear programming, Academic Press, New York, 1970.

[46] R.C. Reid, J.M. Prausnitz, and T.K. Sherwood, The properties of gases and liquids, McGraw-Hill, New York, 3rd. edition, 1977.

[47] R.C. Reid, J.M. Prausnitz, and T.K. Sherwood, The properties of gases and liquids, McGraw-Hill, New York, 4th. edition, 1987.

[48] H. Renon and J.M. Prausnitz, Local compositions in thermodynamic excess functions for liquid mixtures, *AIChE J.*, 14(1):135, 1968.

[49] H. Renon and J.M. Prausnitz, Estimation of parameters for the NRTL equation for excess Gibbs energies of strongly nonideal liquid mixtures, *I&EC Proc. Des. Dev.*, 8(3):413, 1969.

[50] R.V. Sanderson and H.H.Y. Chien, Simultaneous chemical and phase equilibrium calculation, *Ind. Eng. Chem. Proc. Des. Dev.*, 12(1):81, 1973.

[51] W.D. Seider, R. Gautam, and C.W. White, III, Computation of phase and chemical equilibrium: A review, In *Computer Applications to Chemical Engineering*, page 115. American Chemical Society, 1980, ACS Symp. Ser., No. 124(5).

[52] W.R. Smith and R.W. Missen, Chemical Reaction equilibrium analysis: theory and algorithms, Wiley & Sons, 1982.

[53] M.E. Soares, A.G. Medina, C. McDermott, and N. Ashton, Non-Uniqueness in phase and reaction equilibrium computations, *Chem. Eng. Sci.*, 37(4):521, 1982.

[54] D.R. Stull, E.F. Westrum, and G.C. Sinke, The chemical thermodynamics of organic compounds, Wiley and Sons, New York, 1969.

[55] A.C. Sun and W.D. Seider, Homotopy-continuation algorithm for global optimization, In *Recent advances in global optimization*, page 561. Princeton University Press, 1992.

[56] A.C. Sun and W.D. Seider, Homotopy-continuation for stability analysis in the global minimization of the Gibbs free energy, *Fluid Phase Equilibria*, 1994, In Press.

[57] I. Suzuki, H. Komatsu, and M. Hirata, Formulation and prediction of quaternary vapor-liquid equilibria accompanied by esterification, *J. Chem. Eng. Japan*, 3(2):152, 1969.

[58] D.J. Swank and J.C. Mullins, Evaluation of methods for calculating liquid-liquid phase-splitting, *Fluid Phase Equilibria*, 30:101, 1986.

[59] F. van Zandijcke and L. Verhoeye, The vapor-liquid equilibrium of ternary systems with limited miscibility at atmospheric pressure, *J. appl. Chem. Biotechnol.*, 24:709, 1974.

[60] V. Visweswaran and C.A. Floudas, A global optimization algorithm (GOP) for certain classes of nonconvex NLPs: II. Application of theory and test problems, *Comput. chem. engng.*, 14(12):1419, 1990.

[61] V. Visweswaran and C.A. Floudas, Unconstrained and constrained global optimization of polynomial functions in one variable, *Journal of Global Optimization*, 2(12):73, 1992.

[62] V. Visweswaran and C.A. Floudas, New properties and computational improvement of the GOP algorithm for problems with quadratic objective function and constraints, *Journal of Global Optimization*, 3(3):439, 1993.

[63] F.F.Y. Walraven and P.V. van Rompay, An improved phase-splitting algorithm, *Comput. chem. engng.*, 12(8):777, 1988.

[64] C.W. White and W.D. Seider, Computation of phase and chemical equilibrium – Part IV. approach to chemical equilibrium, *AIChE J.*, 27(3):466, 1981.

[65] W.B. White, S.M. Johnson, and G.B. Dantzig, Chemical equilibrium in complex mixtures, *J. Chem. Phys.*, 28(5):751, 1958.

[66] W. Xiao, K. Zhu, W. Yuan, and H.H. Chien, An algorithm for simultaneous chemical and phase equilibrium calculation, *AIChE J.*, 35(11):1813, 1989.

Appendix A

This Appendix shows how global lower and upper bounds can be automatically generated for the x variables $\{\Psi_i^k\}$, which are linear fractional functions. In what follows, the phase superscript k is dropped. The problem is then:

$$\min\ \Psi_i \;=\; \frac{n_i}{\sum\limits_j \mathcal{G}_{ji} n_j}$$

$$\begin{aligned} s.t. \qquad \mathcal{L}_{n_j} - n_j &\le 0 \quad \rightarrow \mu_j^L \qquad \forall\ j \in C \\ n_j - \mathcal{U}_{n_j} &\le 0 \quad \rightarrow \mu_j^U \qquad \forall\ j \in C \end{aligned}$$

where $\{\mathcal{L}_{n_i}, \mathcal{U}_{n_i}\}$ are the lower and upper box bounds on the mol number variables, and $\{\mu_i^L\}$ and $\{\mu_i^U\}$ are the multipliers associated with the corresponding inequality constraints. Recall that $\mathcal{G}_{ji} > 0$. The KKT conditions yield:

$$\frac{1}{\sum\limits_j \mathcal{G}_{ji} n_j} \cdot \left[e_j - \frac{\mathcal{G}_{ji} n_i}{\sum\limits_j \mathcal{G}_{ji} n_j} \right] + \mu_j^U - \mu_j^L \;=\; 0 \quad \forall\ j \in C \tag{A.1}$$

$$\mu_j^L \cdot \left[\ \mathcal{L}_{n_j} - n_j \right] \;=\; 0 \quad \forall\ j \in C \tag{A.2}$$

$$\mu_j^U \cdot \left[\ n_j - \mathcal{U}_{n_j} \right] \;=\; 0 \quad \forall\ j \in C \tag{A.3}$$

$$\mu_j^L\ ,\ \mu_j^L \;\ge\; 0 \quad \forall\ j \in C \tag{A.4}$$

where $e_j = 1$ if $j = i$, and $e_j = 0$ otherwise.

If any n_j lies in the interior of the box constraints, then both multipliers must be zero, i.e. $\mu_j^L = \mu_j^j = 0$ in order to satisfy Eqns. (A.2) and (A.3). However this would imply violation of Eqn. (A.1) so the variables must be at either their lower or upper bounds. It will now be shown how it can be decided *a priori* at what bounds the mol number variables should be set to ensure the x variables attain their global lower and upper bounds within the defined box region.

By examining the sign of the term in square brackets of Eqn. (A.1), it is possible to determine for each j that one of the bounding inequality constraints must be active, while the other cannot. There are two cases for which the analysis is performed:

Case I: $j = i$

$$\text{When} \quad j = i \quad \text{then} \quad \left[e_j - \frac{\mathcal{G}_{ji} n_i}{\sum\limits_j \mathcal{G}_{ji} n_j} \right] \;=\; \frac{\sum\limits_{j \neq i} \mathcal{G}_{ji} n_j}{\sum\limits_j \mathcal{G}_{ji} n_j} \;>\; 0$$

This term is always positive so that μ_j^L must be nonzero to satisfy Eqn. (A.1). Eqn. (A.2) implies that $n_j = \mathcal{L}_{n_j}$. Then, Eqn. (A.3) shows that $n_j - \mathcal{U}_{n_j} < 0$ so that $\mu_i^U = 0$. Thus, when $j = i$, n_j must be at its lower bound if Ψ_i is to be minimized.

Case II: $j \neq i$

$$\text{When} \quad j \neq i \quad \text{then} \quad \left[e_j - \frac{\mathcal{G}_{ji} n_i}{\sum_j \mathcal{G}_{ji} n_j} \right] \; = \; -\frac{\mathcal{G}_{ji} n_i}{\sum_j \mathcal{G}_{ji} n_j} \; < \; 0$$

This term is always negative implying that μ_j^U must be nonzero to satisfy Eqn. (A.1). Eqn. (A.3) implies that $n_j = \mathcal{U}_{n_j}$. Eqn. (A.2) reveals that $\mathcal{L}_{n_j} - n_j < 0$ so that $\mu_i^L = 0$. Thus, for the case $j \neq i$, n_j must be at its upper bound in order to minimize Ψ_i.

Therefore, the global lower bound for any variable Ψ_i constrained within the box bounds $\{\mathcal{L}_{n_i}, \mathcal{U}_{n_i}\}$ is given by:

$$\min \Psi_i = \frac{\mathcal{L}_{n_i}}{\mathcal{L}_{n_i} + \sum_{j \neq i} \mathcal{G}_{ji} \, \mathcal{U}_{n_j}} \tag{A.5}$$

A similar analysis to obtain the maximum of Ψ_i by minimizing $-\Psi_i$ subject to the same box constraints yields the global maximum as:

$$\max \Psi_i \;\equiv\; \min \; -\Psi_i \;=\; \frac{\mathcal{U}_{n_i}}{\mathcal{U}_{n_i} + \sum_{j \neq i} \mathcal{G}_{ji} \, \mathcal{L}_{n_j}} \tag{A.6}$$

In this manner, the global lower and upper bounds on the x variables can be obtained for any given box bounds on the mol number variables. $\square$

Solution for n-Butyl-Acetate (1) – Water (2) $T = 298\text{K}$, $P = 1.0$ atm				
Components	Feed (mols)	Liquid I (mols)	Liquid II (mols)	$\hat{G}_I^*$ (—)
$C_6H_{12}O_2$ (1)	0.50	0.00071	0.49929	-0.02020
H_2O (2)	0.50	0.15588	0.34412	(Global minimum)
$C_6H_{12}O_2$ (1)	0.50	0.00213	0.49787	-0.01961
H_2O (2)	0.50	0.46547	0.03453	(Local minimum)
$C_6H_{12}O_2$ (1)	0.50	0.00173	0.49827	-0.01730
H_2O (2)	0.50	0.37544	0.12456	(Local maximum)

Table 1: Solutions for Illustrative Example

	Parent region information						Multiplier levels			
Iteration	$\mathcal{L}^R_{n_1}$	$\bar{n}_1$	$\mathcal{U}^R_{n_1}$	$\mathcal{L}^R_{n_2}$	$\bar{n}_2$	$\mathcal{U}^R_{n_2}$	$\bar{\lambda}_1$	$\bar{\lambda}_2$	$\bar{\lambda}_1^{II}$	$\bar{\lambda}_2^{II}$
1	0	0.25	0.5	0	0.25	0.5	-0.6436	-0.7075	-0.6436	-0.7075
2	0.25	0.5	0.5	0.25	0.5	0.5	-0.6436	-0.7075	0	0
3	0	0.1028	0.25	0.25	0.3972	0.5	-1.7848	-0.2219	-0.1855	-1.6323
4	0.25	0.3796	0.5	0.25	0.3704	0.5	-0.6302	-0.7207	-0.6853	-0.6687

Table 2: Primal information for Illustrative Example

	Liquid phase I				Liquid phase II			
Region	$\mathcal{L}^B_{\Psi_1}$	$\mathcal{U}^B_{\Psi_1}$	$\mathcal{L}^B_{\Psi_2}$	$\mathcal{U}^B_{\Psi_2}$	$\mathcal{L}^B_{\Psi_1^{II}}$	$\mathcal{U}^B_{\Psi_1^{II}}$	$\mathcal{L}^B_{\Psi_2^{II}}$	$\mathcal{U}^B_{\Psi_2^{II}}$
1	0.7587	0.9263	0.6189	0.8666	0	1	0	1
2	0	0.8628	0.7646	1	0.8628	1	0	0.7646

Table 3: x variable bounds for Iteration 1

	Liquid Phase I				Liquid Phase II			
Region	$\hat{\Psi}_{11}$	$\hat{\Psi}_{12}$	$\hat{\Psi}_{21}$	$\hat{\Psi}_{22}$	$\hat{\Psi}_{11}^{II}$	$\hat{\Psi}_{12}^{II}$	$\hat{\Psi}_{21}^{II}$	$\hat{\Psi}_{22}^{II}$
1	0.9263	0.7587	0.6189	0.8666	0	1	1	0
2	0	0	1	1	1	1	0	0

Table 4: x variable levels for Iteration 1

	Box bounds				Solutions		
Region	$\mathcal{L}_{n_1}^B$	$\mathcal{U}_{n_1}^B$	$\mathcal{L}_{n_2}^B$	$\mathcal{U}_{n_2}^B$	n_1^*	n_2^*	μ^*
1	0.1028	0.25	0.3972	0.5	0.25	0.4775	-0.0778
2	0	0.1028	0.3972	0.5	0.0315	0.4541	-0.0803
3	0.1028	0.25	0.25	0.3972	0.1828	0.3712	-0.0551
4	0	0.1028	0.25	0.3972	0.0226	0.25	-0.1086

Table 5: Relaxed dual information for Iteration 3

	Box bounds				Solutions		
Region	$\mathcal{L}_{n_1}^B$	$\mathcal{U}_{n_1}^B$	$\mathcal{L}_{n_2}^B$	$\mathcal{U}_{n_2}^B$	n_1^*	n_2^*	μ^*
1	0.3796	0.5	0.3704	0.5	0.4416	0.4333	-0.1095
2	0.25	0.3796	0.3704	0.5	0.2563	0.3989	-0.0861
3	0.3796	0.5	0.25	0.3704	0.4173	0.25	-0.0925
4	0.25	0.1028	0.25	0.3704	0.3144	0.3105	-0.0456

Table 6: Relaxed dual information for Iteration 4

Iteration	M^L	$P(\bar{\mathbf{n}})$
1	-0.42615	-0.01758
2	-0.23027	0.00507
3	-0.22209	-0.01754
4	-0.10955	-0.01752
47	-0.02501	-0.01980
73	-0.02169	-0.01988
86	-0.02082	-0.02002
90	-0.02048	-0.02018
92	-0.02039	-0.02019
107	-0.02020	-0.02020

Table 7: Progress of bounds for Illustrative Example

Solution for Toluene (1) – Water (2) $T = 298\text{K},\ P = 1.0$ atm				
Components	Feed (mols)	Liquid I (mols)	Liquid II (mols)	$\hat{G}_I^*$ (—)
C_7H_8 (1)	0.50	0.00005	0.49995	-0.00127
H_2O (2)	0.50	0.49872	0.00128	(Global minimum)

Table 8: Global Solution for Example 1

Toluene (1) – Water (2) – Aniline (3): τ_{ij} and α_{ij} dimensionless					
Components ij	i	j	τ_{ij}	τ_{ji}	$\alpha_{ij} = \alpha_{ji}$
C_7H_8 – H_2O	1	2	4.93035	7.77063	0.2485
C_7H_8 – C_6H_7N	1	3	1.59806	0.03509	0.3000
H_2O – C_6H_7N	2	3	4.18462	1.27932	0.3412

Table 9: Binary data for Example 2

Toluene (1) – Water (2) – Aniline (3) Solution: $\hat{G}_I^* = -0.3574$ with $T = 298$K, $P = 1$ atm.			
Component	Liquid I (mols)	Liquid II (mols)	Feed (mols)
C_7H_8 (1)	0.29949	0.00001	0.2995
H_2O (2)	0.06551	0.13429	0.1998
C_6H_7N (3)	0.49873	0.00067	0.4994
Total mols	0.86485	0.13515	0.9987

Table 10: Global solution for Example 2

n-Propanol (1) – n-Butanol (2) – Water (3): τ_{ij} and α_{ij} dimensionless					
Components ij	i	j	τ_{ij}	τ_{ji}	$\alpha_{ij} = \alpha_{ji}$
C_3H_8O – $C_4H_{10}O$	1	2	-0.61259	0.71640	0.30
C_3H_8O – H_2O	1	3	-0.07149	2.7425	0.30
$C_4H_{10}O$ – H_2O	2	3	0.90047	3.51307	0.48

Table 11: Binary data for Example 3

Solutions for n-Propanol (1) – n-Butanol (2) – Water (3) at T, $P = 1$ atm							
Component	Feed (mols)	Liquid I (mols)	Liquid II (mols)	$\hat{G}^*_{II}$ (—)	cpu (sec)	N_I (—)	N_F (%)
C_3H_8O (1)	0.040	0.0049	0.0351	-1.24112	6.27	313	67
$C_4H_{10}O$ (2)	0.160	0.0095	0.1505				
H_2O (3)	0.800	0.4153	0.3847				
C_3H_8O (1)	0.148	0.1280	0.0200	-1.1919716	29.95	1490	27
$C_4H_{10}O$ (2)	0.052	0.0456	0.0064				
H_2O (3)	0.800	0.6549	0.1451				

Table 12: Global solutions for Example 3

Ethanol (1) – Ethyl Acetate (2) – Water (3) g_{ij} in cal/mol ($\tau_{ij} = g_{ij}/RT$ and α_{ij} dimensionless					
Components ij	i	j	$g_{ij} - g_{jj}$	$g_{ji} - g_{ii}$	$\alpha_{ij} = \alpha_{ji}$
C_2H_6O – $C_4H_8O_2$	1	2	-480.377	1148.848	0.10
C_2H_6O – H_2O	1	3	-53.732	1166.524	0.30
$C_4H_8O_2$ – H_2O	2	3	611.817	1869.890	0.30

Table 13: Binary data for Example 4

Solutions for Ethanol (1) – Ethyl Acetate (2) – Water (3) T = 343.15K, P = 1 atm							
Component	Feed (mols)	Liquid I (mols)	Liquid II (mols)	$\hat{G}^*_{II}$ (—)	cpu (sec)	N_I (—)	N_F (%)
C_2H_6O (1)	0.040	0.0165	0.0235	-1.07738	3.02	153	72
$C_4H_{10}O$ (2)	0.300	0.0382	0.2618				
H_2O (3)	0.660	0.5319	0.1281				

Table 14: Global solution for Example 4

n-Butanol (1) – Water (2) – n-Butyl Acetate (3): τ_{ij} and α_{ij} dimensionless					
Components ij	i	j	τ_{ij}	τ_{ji}	$\alpha_{ij} = \alpha_{ji}$
$C_4H_{10}O$ – H_2O	1	2	0.90047	3.51307	0.48
$C_4H_{10}O$ – $C_6H_{12}O$	1	3	1.15161	-0.30827	0.30
H_2O – $C_6H_{12}O$	2	3	5.04652	1.75717	0.34

Table 15: Binary data for Example 5

n-Butanol (1) – Water (2) – n-Butyl-Acetate (3) Solution: $\hat{G}^*_{II} = -0.91601$ at T, $P = 1$ atm			
Component	Liquid I (mols)	Liquid II (mols)	Feed (mols)
$C_4H_{10}O$ (1)	0.13603	0.00397	0.140
H_2O (2)	0.16661	0.47339	0.640
$C_6H_{12}O_2$ (3)	0.21891	0.00109	0.220
Total mols	0.52155	0.47845	1.000

Table 16: Global solution for Example 5

Benzene (1) – Acetonitrile (2) – Water (3)								
Components ij	i	j	$g_{ij} - g_{jj}$		$g_{ji} - g_{ii}$		$\alpha_{ij} = \alpha_{ji}$	
			300K	333K	300K	333K	300K	333K
$C_6H_6 - CH_3N$	1	2	693.61	998.2	92.47	65.74	0.67094	0.88577
$C_6H_6 - H_2O$	1	3	3892.44	3883.2	3952.2	3849.57	0.23906	0.24698
$CH_3N - H_2O$	2	3	415.38	363.57	1016.28	1262.4	0.20202	0.3565

Table 17: Binary data for Example 6

Solutions for Benzene (1) – Acetonitrile (2) – Water (3) T = 333K, P = 0.769 atm					
Components	Feed (mols)	Liquid I (mols)	Liquid II (mols)	Vapor (mols)	$\hat{G}^*_{II}$ (—)
C_6H_6 (1)	0.34483	0.23946	0.00073	0.10464	-1.40852
C_2H_3N (2)	0.31034	0.22701	0.02169	0.06163	(Global LLV)
H_2O (3)	0.34843	0.03365	0.26235	0.05242	
C_6H_6 (1)	0.34483	0.00096	(—)	0.34387	-1.39785
C_2H_3N (2)	0.31034	0.02416	(—)	0.28618	(Local LV)
H_2O (3)	0.34843	0.15562	(—)	0.19281	

Table 18: Solutions for Example 6: Conditions (A)

Solution for Benzene (1) – Acetonitrile (2) – Water (3) T = 333K, P = 1.0 atm				
Components	Feed (mols)	Liquid I (mols)	Liquid II (mols)	$\hat{G}^*_{II}$ (—)
C_6H_6 (1)	0.34483	0.34401	0.00082	-1.40782
C_2H_3N (2)	0.31034	0.28651	0.02383	(Global LL)
H_2O (3)	0.34843	0.03785	0.31058	

Table 19: Global solution for Example 6: Conditions (B)

Solutions for Benzene (1) – Acetonitrile (2) – Water (3) $T = 300$K, $P = 0.10$ atm					
Components	Feed (mols)	Liquid I (mols)	Liquid II (mols)	Vapor (mols)	$\hat{G}^*_{II}$ (—)
C_6H_6 (1)	0.34483	0.000003	(—)	0.344827	-3.41234
C_2H_3N (2)	0.31034	0.000490	(—)	0.309850	(Global LV)
H_2O (3)	0.34843	0.015858	(—)	0.332572	
C_6H_6 (1)	0.34483	0.34431	0.00052	(—)	-2.86435
C_2H_3N (2)	0.31034	0.28569	0.02465	(—)	(Local LL)
H_2O (3)	0.34843	0.03310	0.31533	(—)	

Table 20: Solutions for Example 6: Conditions (C)

Ethanol (1) – Acetic Acid (2) – Ethyl Acetate (3) – Water (4)				
τ_{ij}	$EtOH$	HAc	$EtAc$	H_2O
$EtOH$	0.0	1.3941	0.6731	-0.2019
HAc	-1.0182	0.0	0.0070	-0.4735
$EtAc$	0.1652	0.5817	0.0	1.7002
H_2O	2.1715	1.6363	1.9257	0.0

Table 21: Binary data for Example 7

Data for the elemental mass constraints					
a_{ei}	$EtOH$	HAc	$EtAc$	H_2O	b_e
C	2	2	4	0	2.0
H	6	4	8	2	5.0
O	1	2	2	1	1.5

Table 22: Elemental abundance parameters for Example 7

Ethanol (1) – Acetic Acid (2) – Ethyl Acetate (3) – Water (4) Solution: $\hat{G}^* = -90.7795$ with $T = 355$K, $P = 1$ atm.			
Component	Liquid (mol fraction)	Vapor (mol fraction)	$\Delta G_i^{V,f}$ (cal/mol)
$EtOH$ (1)	0.03980	0.07830	−37.0918
HAc (2)	0.20181	0.06984	−87.3031
$EtAc$ (3)	0.08163	0.44147	−72.8406
H_2O (4)	0.67676	0.41038	−54.0234
Total mols	0.04964	0.95036	(—)

Table 23: Global solution for Example 7 at T=355K

Ethanol (1) – Acetic Acid (2) – Ethyl Acetate (3) – Water (4) Solution: $\hat{G}^* = -89.8003$ with $T = 358$K, $P = 1$ atm.			
Component	Liquid (mol fraction)	Vapor (mol fraction)	$\Delta G_i^{V,f}$ (cal/mol)
$EtOH$ (1)	(—)	0.075313	−36.9228
HAc (2)	(—)	0.075313	−87.1561
$EtAc$ (3)	(—)	0.424687	−72.5494
H_2O (4)	(—)	0.424687	−53.9903
Total mols	0.0	1.0	(—)

Table 24: Global solution for Example 7 at T = 358K

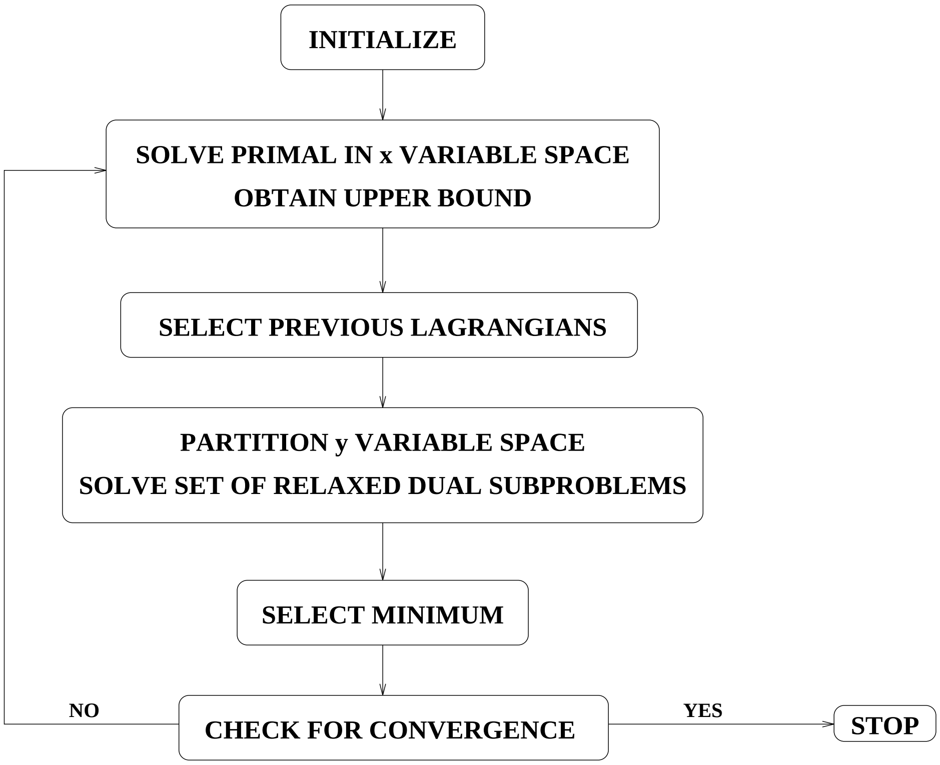

Figure 1: Conceptual outline of the GOP algorithm

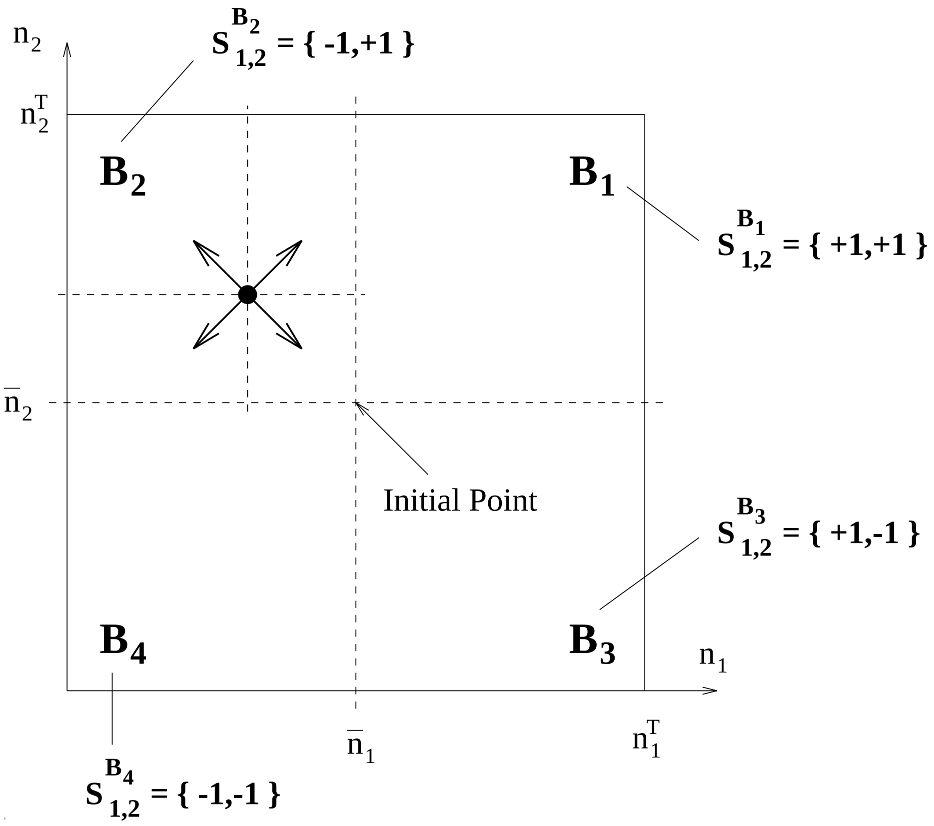

Figure 2: Example for two connected variables

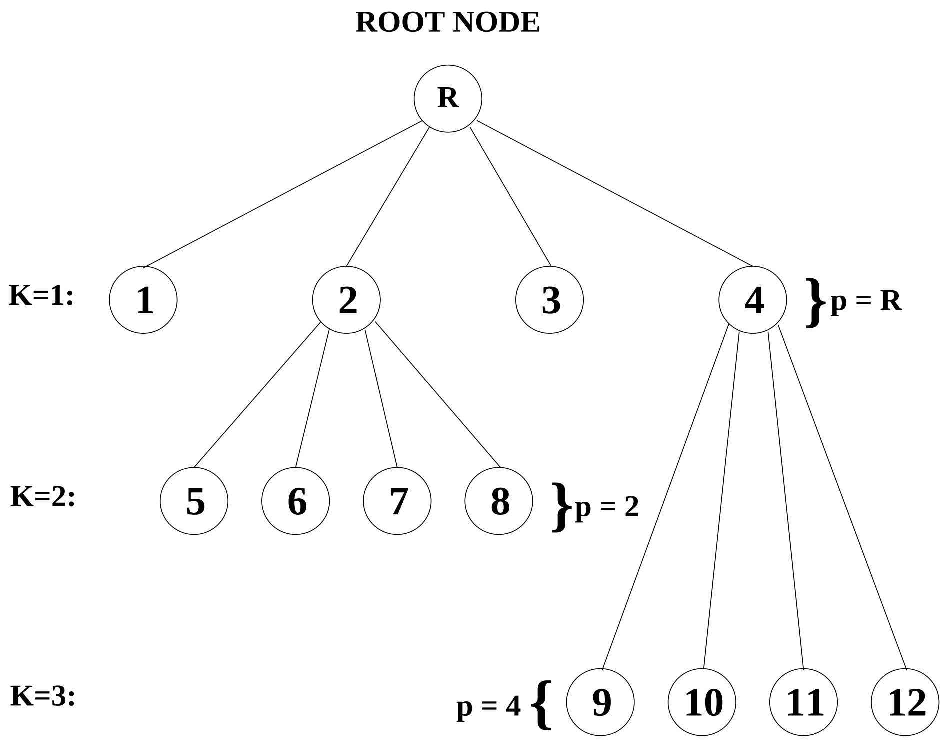

Figure 3: Tree structure for solution storage

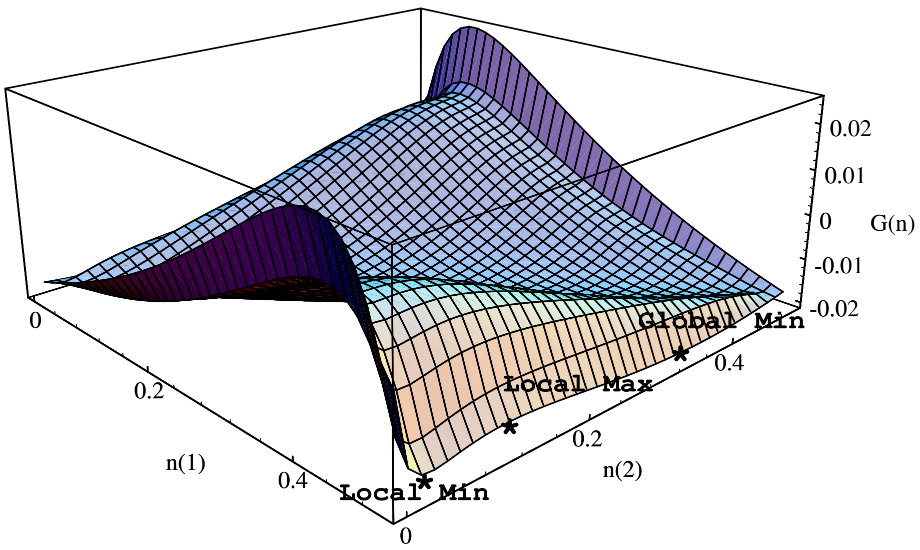

Figure 4: Gibbs energy surface for Illustrative Example

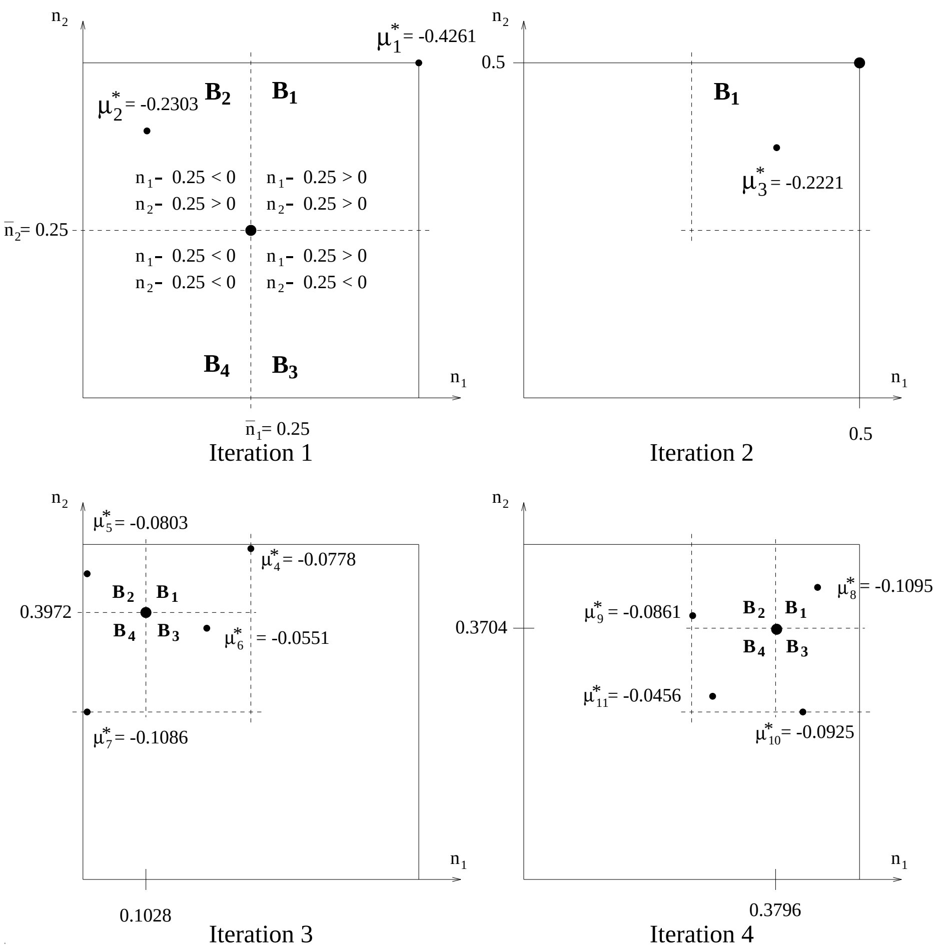

Figure 5: Box region and solution locations in the y variable space

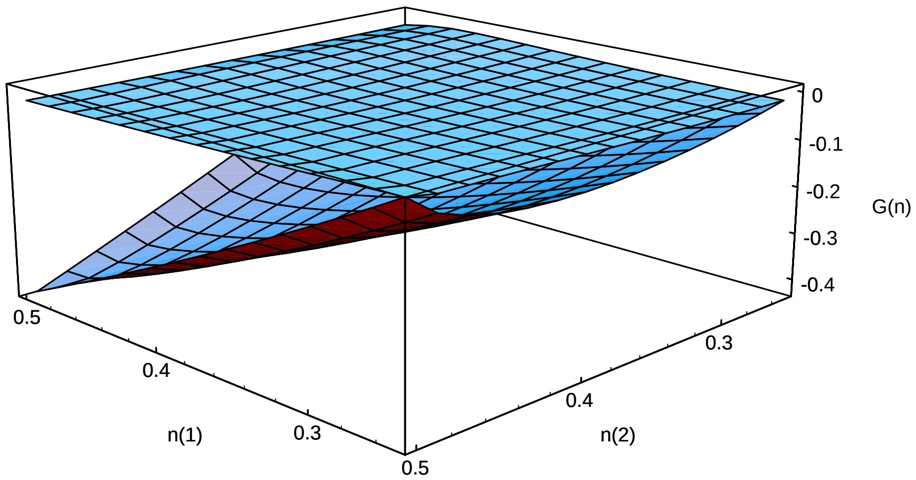

Figure 6: Gibbs surface and Lagrangian for Region 1 of Iteration 1

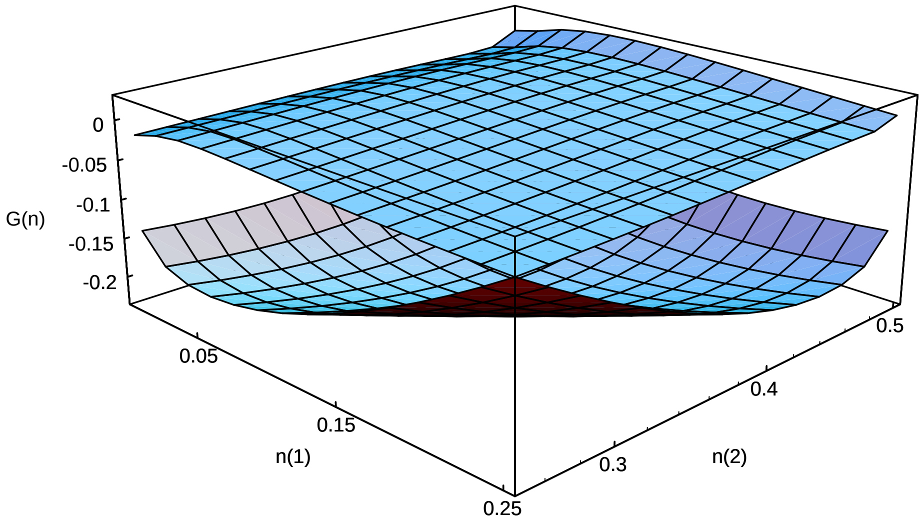

Figure 7: Gibbs surface and Lagrangian for Region 2 of Iteration 1

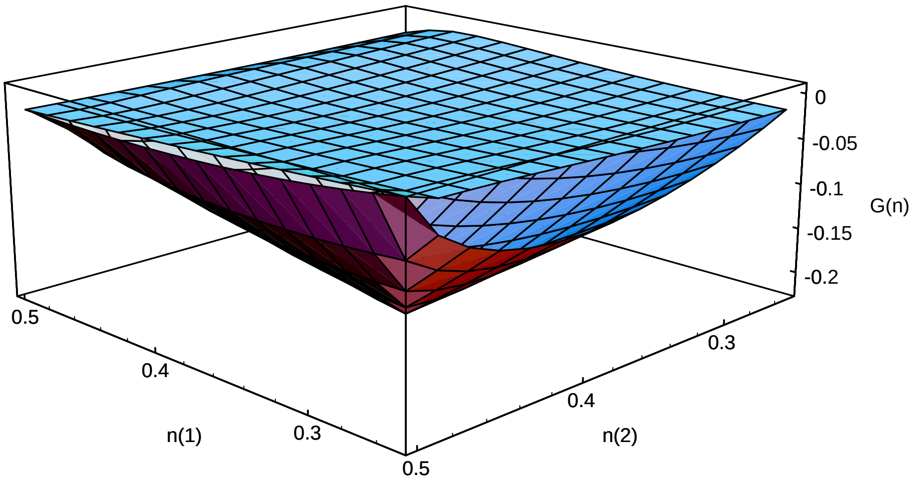

Figure 8: Gibbs surface and Lagrangian for Iteration 2

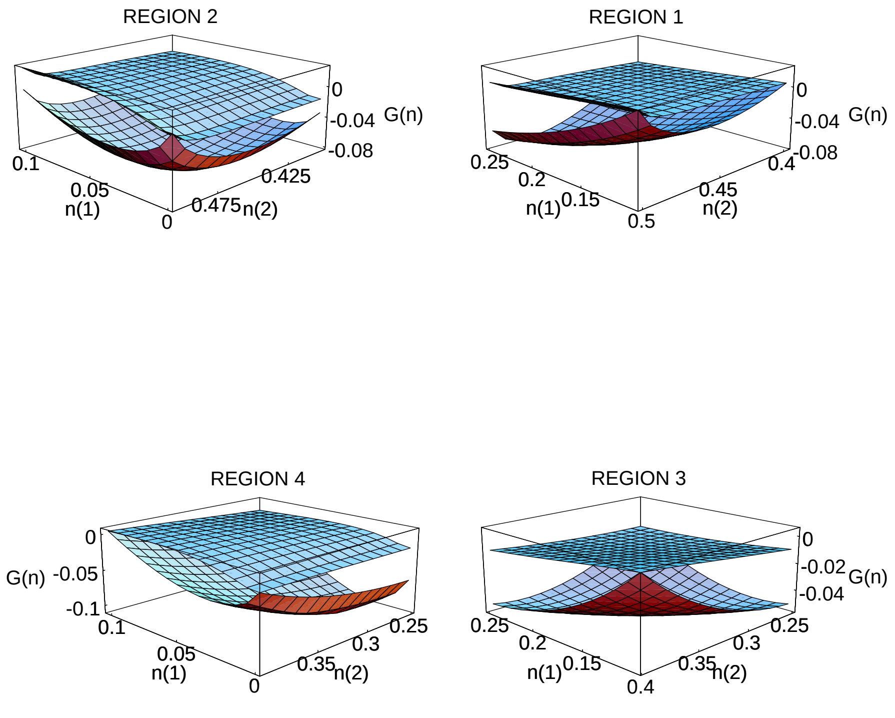

Figure 9: Gibbs surfaces and Lagrangians for Iteration 3